THESIS

GENOMIC DIVERSITY AND RELATEDNESS IN THE FOUNDING BLACK-FOOTED FERRET POPULATION

Submitted by

Robyn L Bortner

Department of Biology

In partial fulfillment of the requirements

For the Degree of Master of Science

Colorado State University

Fort Collins, Colorado

Summer 2026

Master's Committee:

Advisor: Michael Antolin

Klaus-Peter Koepfli
Jennifer Barfield

ABSTRACT

GENOMIC DIVERSITY AND RELATEDNESS IN THE FOUNDING BLACK-FOOTED FERRET POPULATION

Black-footed ferrets (*Mustela nigripes*) are small obligate carnivores native to North American prairie ecosystems. They have the unfortunate but notable distinction of being assumed extinct twice in their history. Depending on healthy prairie dog (*Cynomys* spp.) colonies for both food and shelter, black-footed ferrets most likely declined in response to prairie habitat loss and fragmentation, prairie dog eradication programs, and non-native disease, most notably sylvatic plague (caused by the bacterium *Yersinia pestis*). After their rediscovery at a single site in Wyoming in 1981, a successful captive-breeding and reintroduction effort was established using the last 18 living individuals. Of these, only seven are considered to be genetic founders of all remaining black-footed ferrets. Coupled with the last wild population being isolated on the far western edge of the species range, the founding black-footed ferrets had likely experienced a severe genetic bottleneck. Genetic management of the captive breeding population has been largely achieved through pedigree analysis. Although studied prior to capture, the founders were assumed to be unrelated as they were all wild-caught, and paternity was assumed based upon proximity when captured. As they were all captured from the same dwindling source population, their relationships to each other are likely more complicated than studbook assumptions suggest. Fortunately, suitably preserved samples existed for 19 individuals of the source population, including the seven assumed founders. We used next generation sequencing data and bioinformatics focused on genomic variant discovery to characterize the amount of variation in

the founders, estimate levels of relatedness among the sampled individuals, infer relationships, and compare to the current captive breeding population. We found low levels of genome-wide heterozygosity and high proportions of the genome in runs of homozygosity. Results confirmed some assumed relationships within the source population but contradicted others. Analysis also suggests that the founding population had a (not unexpected) higher level of background relatedness than initially assumed. This work will inform further genetic investigation and conservation of the species both in captive breeding and in establishing viable wild populations.

ACKNOWLEDGMENTS

I would like to thank the following people for their help with this project:

The curators and staff at the Museum of Southwest Biology at the University of New Mexico and the Museum of Vertebrate Biology at the University of California, Berkeley, for the generous loan of black-footed ferret tissues from the Meeteetse population, without which this project would not have been possible. Colorado State University and the U.S Fish & Wildlife Service for funding and support. My advisor, Dr. Michael Antolin, for thoughtfully guiding me through this process at a non-traditional time in my life, and my committee members Dr. Klaus-Peter Koepfli and Dr. Jennifer Barfield for their support and feedback. The staff at the USFWS National Black-footed Ferret Conservation Center and Regional Office for supporting me through this journey, and Pete Gober, who set me on a path I probably would not have found on my own. Dean Biggins along with Steve Forrest and Dave Seery for sharing their invaluable experiences with the ferret populations at Meeteetse. My coworker Morgan Dubois for lending her map-making skills, and my fellow graduate student Jessie Mader, without whom statistics would have been a lonelier journey. And all my friends and family for helping along the way.

TABLE OF CONTENTS

LIST OF TABLES

LIST OF FIGURES

CHAPTER 1: INTRODUCTION

1.1 Background

The black-footed ferret (*Mustela nigripes;* hereafter, black-footed ferret, or ferret) is a nocturnal and fossorial mustelid native to North America. Its closest living relative is the steppe polecat (*Mustela eversmanii*), and it likely diverged from Eurasian ancestors after crossing Beringia during the Pleistocene (Wisely et al. 2008). Once in North America black-footed ferrets became obligate carnivores primarily of prairie dogs (*Cynomys spp*; Sheets et al. 1972; Campbell et al. 1987), and are reliant on healthy colonies for both food and shelter, where ferrets spend much of their time underground. Ferrets are solitary except for breeding or raising young, which occurs in spring, and litters may remain with their mothers until old enough to disperse in fall or early winter; young-of-the-year are capable of breeding the following spring. Historically the black-footed ferret's range coincided with that of the four species of prairie dog on the Great Plains and in intermontane regions of the Rocky Mountains north to Canada and as far south as northern Mexico (Anderson et al. 1986).

Ferret populations declined throughout the 1900s with the reduction of prairie dog habitat (Anderson et al. 1986) driven by the westward expansion of agriculture and development that brought habitat loss, fragmentation, and non-native disease. Prairie dogs were routinely eradicated as agricultural pests, reducing and fragmenting habitat as agriculture and cattle ranching expanded. Unlike their Eurasian ancestors and some other carnivores, black-footed ferrets are exquisitely sensitive to sylvatic plague (caused by the bacterium *Yersinia pestis*) as well as infection by the canine distemper virus (CDV) (Williams et al. 1988; Williams et al.

1994). Now present in every state in the black-footed ferret's historic range, plague continues to be a primary challenge to recovery (U.S. Fish and Wildlife Service 2013).

Black-footed ferrets have the notorious distinction of being assumed extinct twice in their history. First described by Audubon in 1851 (Anderson et al. 1986), ferrets were rare and assumed to be potentially extinct by the 1950s. A population was found in Mellette county, South Dakota in 1964 (Hillman 1968). A captive breeding effort was mounted but ultimately failed; the last wild ferrets in South Dakota were detected in 1974, and the last captive animals died in 1979, after which they were presumed extinct for the second time (U.S. Fish and Wildlife Service 2013).

Black-footed ferrets were rediscovered in 1981 in a remote prairie dog colony west of the small town of Meeteetse, Wyoming (Forrest et al. 1988) when, as the story goes, a ranch dog encountered one near his home. Initially studied by biologists, the population started to decline and the decision was made to bring animals in for a captive breeding effort. By 1987 the last 18 confirmed living ferrets had been trapped, and the wild population died out. The first captive-born offspring were born that same year.

Since then, more than 12,000 black-footed ferrets have been born into a multi-institutional program, as part of a comprehensive recovery program led by the USFWS National Black-footed Ferret Conservation Center. Releases began in 1991 and currently occur annually in the fall, primarily with that year's offspring (U.S. Fish and Wildlife Service 2013). Despite these ongoing efforts, the black-footed ferret remains one of North America's most endangered mammals.

While the rediscovery of this species brought hope for its persistence, it also brought challenges. The last population of ferrets from Meeteetse were on the far western edge of the species range in the Wyoming basin and had likely become isolated from other populations during the Holocene (Wisely et al. 2008) well before the human-driven contraction of the species range in the 1900s. Any other remaining genetic variation in the species was lost with the extirpation of the Great Plains populations.

The population underwent a further bottleneck with the sharp decline of the Meeteetse population during the 1980's. All extant black-footed ferrets known today, both captive and reintroduced, are descended from this small source population. The successful captive breeding population would have been susceptible to founder effects from the limited gene pool with which it was started (Jamieson 2011). Suspected phenotypic effects from this small starting population include reduced semen quality (Santymire et al. 2019) and decreased fecundity (Santymire et al. 2014).

To prevent further loss of genetic diversity, careful genetic management of the captive-breeding population has occurred since its inception. Cooperation with the Association of Zoos & Aquariums (AZA) and the Population Management Center (PMC) allow yearly breeding recommendations focused on prioritizing pairing between individuals with low mean kinship to maximize retention of gene diversity (Baughman et al. 2026). This approach aligns with the idea that conserving genome-wide genetic diversity is the best strategy to avoid inbreeding depression and the loss of nucleotide diversity (π), leading to increased genetic load through inbreeding and

the loss of adaptive potential (Kardos et al. 2021). Almost all breeding population recommendations to date have been informed from pedigree data. Black-footed ferrets have the advantage of a pedigree that is 100% known since its inception. Regardless, pedigrees can only track expected levels of inbreeding and inheritance but cannot account for inbreeding that occurred in ancestors prior to the known pedigree. The breeding history and relationships of the founding ferrets prior to the start of the captive breeding program were largely unknown.

Molecular markers, including microsatellites and single nucleotide polymorphisms (SNPs), have become an essential tool in the field of conservation genomics (Allendorf et al. 2022; Prunier et al. 2023). SNPs in particular have been used to address a wide range of genomic conservation questions such as levels of genetic diversity (Marr et al. 2025), relatedness (Galla et al. 2020), and population structure (Zimmerman et al. 2025). SNPs have also been shown to be better predictors of inbreeding than measures derived from pedigrees, as pedigrees only estimate the average relatedness among descendants (Kardos et al. 2015).

For this project we used next generation (NGS) whole genome resequencing data from samples obtained from 19 of the originally caught Meeteetse ferrets, as well as 5 descendant animals from 1998-2024. Our main questions were:

- What genetic diversity (or lack thereof) did the founding population start with?
- What can we infer about the relationships of the founding ferrets with molecular sequencing data?
- Given the initial assumed pedigree, do we truly have seven founders?

1.2 Founder Population Demographics

The last known black-footed ferrets were found in an isolated population outside of the town of Meeteetse in Park County, Wyoming, on the far western edge of the species' historic range. (Figure 1-1). This Wyoming Basin population was differentiated from other historic ferret populations, with relatively low genetic diversity, and likely existed in isolation after the last glacial maximum (Wisely et al. 2008). The site was comprised of a total of 3100 ha (7660.3 acres) of white-tailed prairie dog (*Cynomys leucurus*) colonies ranging in size from 2.5 to 740 ha (Forrest et al. 1988). Much of the following overview of the Meeteetse population and the 24 captured source population ferrets was obtained via direct conversation with one of the biologists who performed the work, Dean Biggins, and his subsequent conversations with two other researchers from the time, Steve Forrest and Dave Seery.

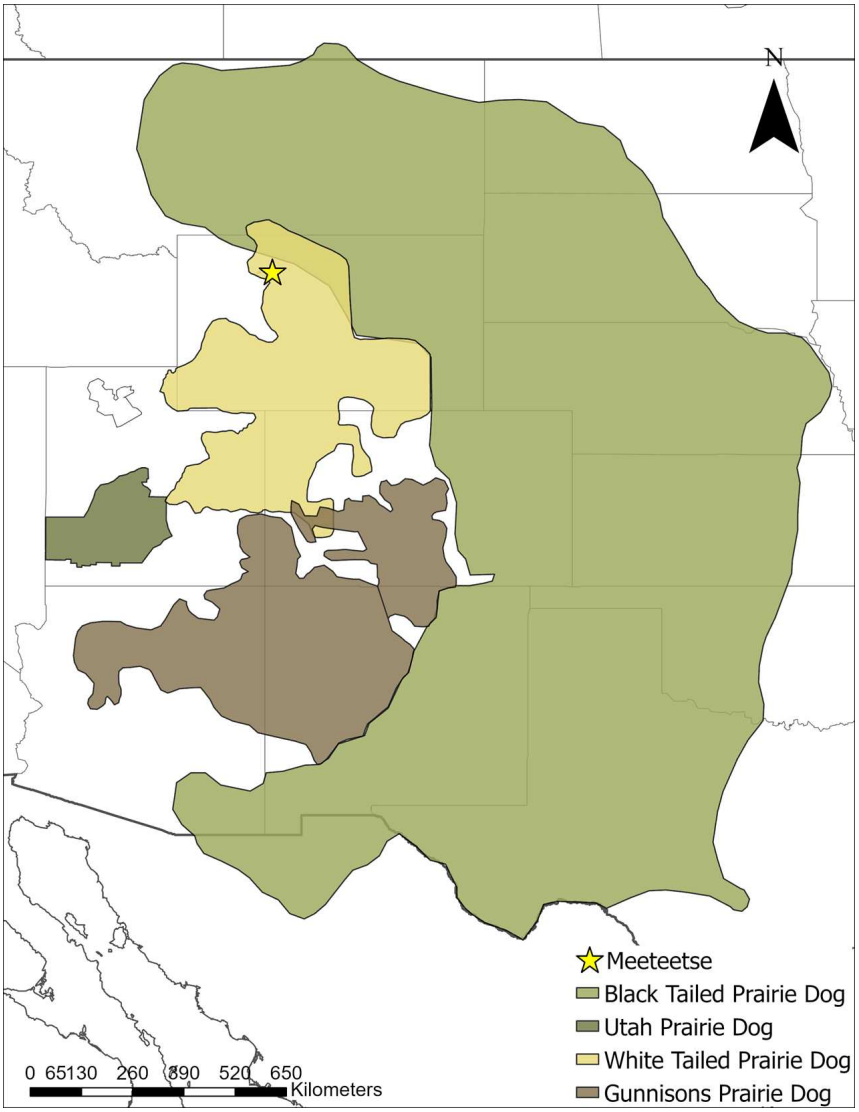

Figure 1-1. Historic range of the four species of prairie dog

Since its discovery in 1981, the population peaked at 129 ferrets after July spotlight surveys in 1984 before dropping to 58 ferrets in 1985. It continued to noticeably decline from July to September 1985 by 47% (Forrest et al. 1988). This decline was attributed at least in part to an outbreak of canine distemper virus (CDV) in the ferret population detected in November of 1985. However, sylvatic plague had also been detected in the prairie dog population in July of 1985 (Forrest et al. 1988; Williams et al. 1988).

Given current knowledge of the susceptibility of the black-footed ferret to plague (Biggins and Godbey 2003; Rocke et al. 2008), it has been surmised that this disease played a larger role in the decline of the Meeteetse population than was thought in the 1980s. Plague was first determined to be fatal to black-footed ferrets in 1993 after a young male at Sybille (the first black-footed ferret breeding facility in Wyoming) contracted it in an outdoor enclosure, presumably from an infected prairie dog. Previously, ferrets were assumed to be resistant to plague based on lack of severe disease in other carnivores and mustelids (Williams et al. 1994). Plague susceptibility was confirmed in 1995 when accidental feeding of plague-infected prairie dog carcasses killed 27 black-footed ferrets at a captive breeding and preconditioning facility near Pueblo, Colorado (Godbey et al. 2006). More recent field studies have documented substantial mortality of non-vaccinated black-footed ferrets compared to their plague-vaccinated counterparts, even when plague circulation was at much lower levels than were occurring during the epizootic at Meeteetse during 1985 (Matchett et al. 2010).

Trapping of ferrets to start a captive-breeding program began in September 1985 with efforts intensifying by summer of 1986 in response to the rapid population decline. A total of 24 individuals were trapped between 1985 and 1987. Locations of prairie dog colonies that existed where ferrets were captured near Meeteetse in 1985 and the approximate trapping locations of the ferrets are shown in Figure 1-2. All ferrets in the breeding program have been assigned a unique studbook number since the inception of trapping from the wild; these will be used to identify ferrets throughout. Ferrets in the Meeteetse population were also identified with physical ear tags and tattoos.

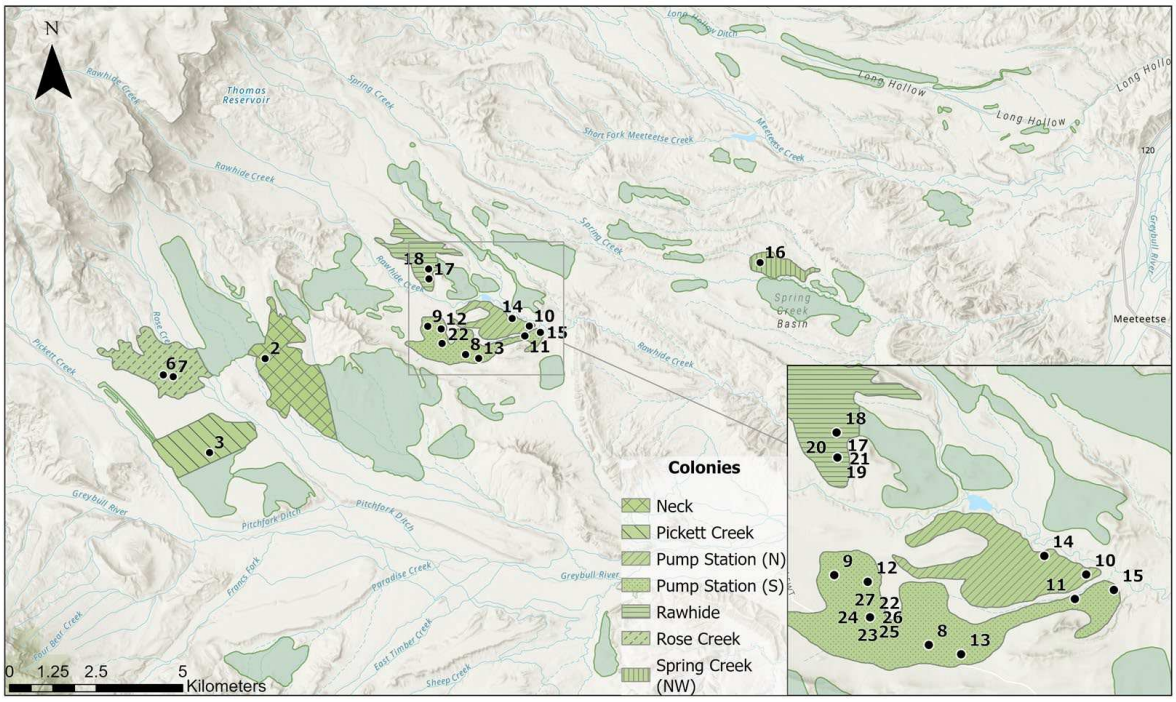

Figure 1-2. Map of Meeteetse prairie dog colonies and ferret trap locations. Ferret trap points are labeled by studbook number, and the relevant prairie dog colonies on which they were found are highlighted. Most of the ferrets were caught within a ~3km radius of each other in the central Rawhide and Pump Station colonies.

A comprehensive list of these animals is presented in Table 1.1. Trapped ferrets were assigned to adult or juvenile age classes with methods from Thorne, et. al. 1985 (Forrest et al. 1988). The first six caught in September and October of 1985 succumbed to infection by CDV (Williams et al. 1988). Ferrets in this first trapping effort included studbook numbers 2, 3, 7, 8, 9, and 15. (Note that SB# 2 was not originally assigned a studbook number but careful cross-referencing has properly identified his sample). These six samples were acquired from the University of California, Berkeley Museum of Vertebrate Zoology; all other Meeteetse samples came from the University of New Mexico Museum of Southwestern Biology).

The next six were caught between October and November 1985. These were placed in isolation at the Sybille facility and did not develop CDV (Williams et al. 1988). These included studbook

numbers 6, 10, 11, 12, 13, and 14. The next 11 were caught in 1986; 3 adults and 2 litters of kits. These include studbook numbers 16, 17, 19, 20, 21, 22, 23, 24, 25 26, and 27. Surveys in November of 1985 had confirmed the presence of at least three adult ferrets but without specific identification, so whether these were all caught is unknown. Studbook number 18 was the last wild black-footed ferret to be trapped in February of 1987; no further individuals were detected.

Table 1.1. The original 24 wild-caught black-footed ferrets.

SB#	Sex	Name	Capture date	Age class	Birth year	Colony Name	Comments
2	M		5-Oct-1985	adult	1984	Neck	initially not assigned a SB#; died of CD
3	F		5-Oct-1985	juv.	1985	Pickett Creek	unconfirmed parents; died of CD
6	F	Molly	31-Oct-1985	juv.	1985	Rose Creek	unconfirmed parents
7	F		5-Oct-1985	juv.	1985	Rose Creek	unconfirmed parents; died of CD
8	F		11-Oct-1985	adult	1983	Pump Station (S)	died of CD
9	M		12-Sep-1985	adult	1984	Pump Station (W)	died of CD
10	F	Willa	2-Nov-1985	adult	1984	Pump Station (N)	
11	F	Emma	29-Oct-1985	adult	1984	Pump Station (N)	
12	F	Annie	25-Oct-1985	adult	1984	Pump Station (W)	
13	M	Dexter	31-Oct-1985	juv.	1985	Pump Station (S)	assumed offspring of SB# 8 and SB# 9
14	M	Cody	25-Oct-1985	juv.	1985	Pump Station (N)	assumed offspring of SB# 10
15	M		12-Sep-1985	juv.	1985	Pump Station (N)	assumed offspring of SB# 11; died of CD
16	M	Dean	27-Jul-1986	adult	1985	Spring Creek	last ferret found in this area
17	F	Jenny	3-Sep-1986	adult	1985	Rawhide	
18	M	Scarface	28-Feb-1987	adult	1985	Rawhide	last ferret caught in 1987
19	F	Becky	11-Aug-1986	juv.	1986	Rawhide	assumed offspring of SB# 17 and 18
20	M	Rocky	3-Sep-1986	juv.	1986	Rawhide	assumed offspring of SB# 17 and 18
21	M	Sundance	1-Sep-1986	juv.	1986	Rawhide	assumed offspring of SB# 17 and 18
22	F	Mom	30-Aug-1986	adult	1985	Pump Station (W)	
23	M	Cutlip	30-Aug-1986	juv.	1986	Pump Station (W)	assumed offspring of SB # 22 and 18
24	F	Collene	30-Aug-1986	juv.	1986	Pump Station (W)	assumed offspring of SB # 22 and 18
25	F	Rene	30-Aug-1986	juv.	1986	Pump Station (W)	assumed offspring of SB # 22 and 18
26	F	Jez	30-Aug-1986	juv.	1986	Pump Station (W)	assumed offspring of SB # 22 and 18
27	F	Amy	30-Aug-1986	juv.	1986	Pump Station (W)	assumed offspring of SB # 22 and 18

Birth years for ferrets determined to be an adult at capture were estimated to the previous spring as ferrets are reproductive at 1 yr of age. Juveniles caught in the fall are estimated to spring of the same year. SB# 8 was tagged and observed as an adult in 1984; therefore, her birth year has been estimated as 1983. (CD is canine distemper).

Notes of interest on particular individuals:

- SB# 8 (F, adult): Caught in the south portion of the Pump Station prairie dog town. She was tracked as an adult with a litter in 1984; her birth year is therefore assumed to be no later than 1983.
- SB# 16 (M, adult): Caught on the Spring Creek town in the far east part of the area, about 7 km from the central prairie dog colonies. Known as 'Dean', he was the last individual to be found here and the only one to be trapped from that area. His more remote location will prove of interest in later analyses.
- SB# 18 (M, adult): The last animal to be caught, known as Scarface, in February of 1987, in the same burrow that SB# 17 (Jenny) had raised her litter in the previous year. He was assumed to be the sire of SB# 17 (Jenny) and 22's (Mom) litters as he was the last mature male to be detected in the area. The success of the initial captive breeding effort is often attributed to his reproductive prowess.

1.3 Pedigree and Assumptions

The Black-footed Ferret Studbook is currently maintained in ZIMS for Studbooks (Species360 Zoological Information Management System (ZIMS) 2026, zims.Species360.org) in cooperation with the Association of Zoos & Aquariums (AZA) Population Management Center (PMC). It was imported into this format from older studbook software known as SPARKS (Single Population Analysis and Records Keeping System) in 2020.

Following the assumptions recorded for the wild-caught source individuals, the ferret captive breeding pedigree is 100% known (Baughman et al. 2026). Every pairing of animals and

resulting offspring have been recorded since the inception of the captive breeding program and includes all known black-footed ferrets in human care. The starting individuals in a studbook are known as founders. By AZA's studbook definition, a founder is "An individual obtained from a source population (often the wild) that has no known relationship to any individuals in the derived population (except for its own descendants)" (Baughman et al. 2026).

The assumed pedigree of the original 24 captured ferrets as entered in the studbook is shown in Figure 1-3. Of these, 13 were in the potential founder generation (i.e. were unique individuals with no known antecedents). Two of these were known as WILD4 and WILD5: hypothetical wild parents assigned to siblings SB# 6 and SB# 7 to indicate their sibling relationship. WILD4 and WILD5 were never captured or held in captivity. The others were SB#s 2, 3, 8, 9, 10, 11, 12, 16, 17, 18, and 22. After the loss of the first six captured ferrets to CDV in 1985, 18 individuals remained alive to start the captive breeding effort. Although breeding in captivity occurred among 15 of these individuals, not all resulting offspring survived to reproduce.

Just seven founders were identified among the Meeteetse source population. These included SB#s 8 and 9, both of whom died of CDV shortly after capture (and are not included in the oft cited 18 to start the population, despite being two of the founders), but whose lineages continued on from the successful breeding of their assumed son, SB# 13 (Dexter). The others were SB# 12 (Annie), SB# 16 (Dean), SB# 17 (Jenny), SB# 18 (Scarface), and SB# 22 (Mom). Note that SB# 3 was identified as a juvenile at time of capture, with wild parents that were never caught but originally listed as SB# 1 and 2. After updates to the studbook in 2015, these no longer align with the SB# 1 and 2 presented here.

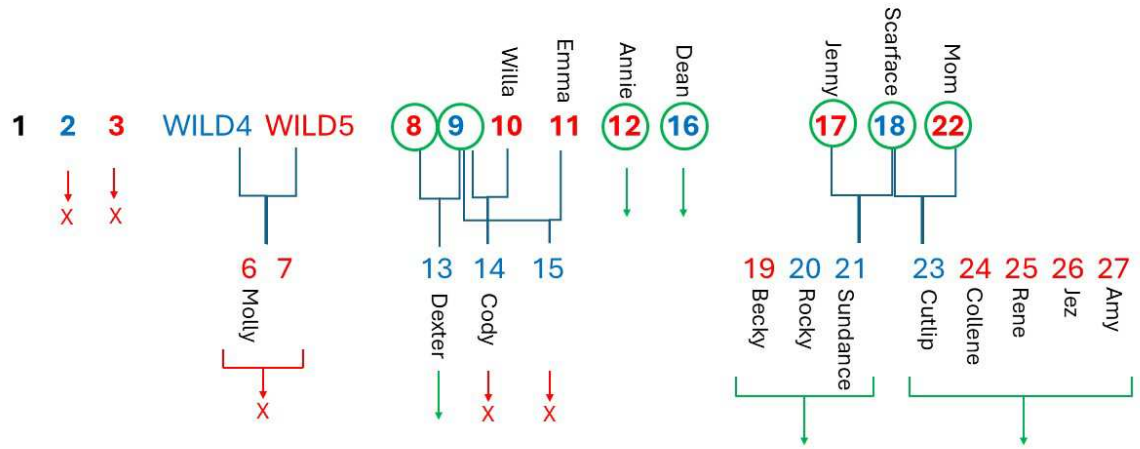

Figure 1-3. Pedigree as entered in the studbook.
Red are females, blue are males. Green circles indicate individuals considered founders. Green arrows indicate lineages that continued to the present day, red arrows are from ferrets that did not successfully reproduce.

Juveniles with SB#s 13, 19, 20, 21, 23, 24, 25, 26, and 27 successfully reproduced in captivity in those early years. However, because their assumed parents were also in the source population, none of them are considered founders for the purposes of the studbook.

All of the first 24 ferrets were wild-caught; none were born in captivity. All their recorded relationships in the studbook are assumptions based on the observations and acquired knowledge of the biologists at the time. Many of these assumptions were made with high confidence and based on thorough observations and knowledge of the species' biology, for instance siblings caught together in the same burrow, or young litters tracked and then caught with their dams. Sire assumptions are, by nature, much less certain. Black-footed ferrets are non-monogamous and the home ranges of both sexes can overlap, with male overlap highest in areas of high female

density (Eads et al. 2014). Males take no part in raising offspring. Sire assumptions were made based on the proximity and behavior of the potential males in the area at the time.

For analytical purposes and to satisfy the requirements of the studbook software, the seven founding individuals have been assumed to be unrelated; that is, have a kinship coefficient (ϕ) or r (2ϕ) of 0. Considering the small, isolated population from which they were caught, this is probably incorrect (Marinari and Lynch 2021). This assumption, along with the assumed pedigree, form the guiding hypotheses for many of the analyses in this project.

CHAPTER 2: METHODS

2.1 Sample Acquisition

Source population samples for this project were acquired from the University of California, Berkeley Museum of Vertebrate Zoology (MVZ) and the University of New Mexico Museum of Southwestern Biology (MSB). Samples are post-mortem museum accessions from frozen muscle or liver tissue. One descendent born in 1998 was also acquired from MVZ, and 4 modern samples were stored as whole blood at the National Black-footed Ferret Conservation Center (FCC) in Carr, Colorado.

2.2 DNA Extraction and Sequencing

DNA extraction, library preparation, and Next Generation Sequencing (NGS) were performed by Psomagen Inc., Rockville, MD. See Table 2.1 for sample accession ID, SB#, Sex, and DNA Integrity Number (DIN) for sample quality control following DNA extraction, and sequencing depth (Coverage).

Table 2.1. List of samples that passed Quality Control (QC). MVZ = University of California, Berkeley Museum of Vertebrate Zoology, MSB = University of New Mexico Museum of Southwestern Biology, FCC = National Black-footed Ferret Conservation Center.

Sample ID	SB#	Sex	Birth Year	DIN	Coverage	Type
MVZ195117	2	M	1984	8.2	30x	Source Population
MVZ195118	3	F	1985	7.8	20x	Source Population
MSB127009	6	F	1985	9.4	20x	Source Population
MVZ195114	7	F	1985	7.8	20x	Source Population
MVZ195115	8	F	1983	8.2	20x	Founder
MVZ195113	9	M	1984	8.4	20x	Founder
MSB122103	12	F	1984	8.2	20x	Founder
MSB127010	13	M	1985	6.2	20x	Source Population
MSB122107	14	M	1985	8.1	20x	Source Population
MVZ195116	15	M	1985	5.9	20x	Source Population
MSB127012	16	M	1985	9.2	20x	Founder
MSB122108	17	F	1985	8.8	20x	Founder
MSB122109	18	M	1985	8.1	20x	Founder
MSB122105	19	F	1986	7.4	20x	Source Population

MSB122104	20	M	1986	6.1	20x	Source Population
MSB122101	21	M	1986	6.7	20x	Source Population
MSB122110	22	F	1985	8.5	20x	Founder
MSB122102	23	M	1986	7	20x	Source Population
MSB127011	25	F	1986	5.2	20x	Source Population
MVZ220147	2320	M	1998	6.8	30x	Descendant
FCC8215	8215	M	2014	9.3	30x	Descendant
FCC8932	8932	F	2017	9.1	30x	Descendant
FCC8934	8934	M	2017	9.1	30x	Descendant
FCC11283	11283	F	2024	9	30x	Descendant

Nineteen samples were sent for sequencing in the first round. One sample (MSB122106, SB#11, Emma) failed QC and returned no useable DNA and was excluded from the study. Six additional samples were sequenced in the second batch. These included two more from MVZ Berkeley: MVZ195117 (original tissue from SB# 2) and MVZ220147 (SB# 2320, a captive population animal born in 1998), and 4 modern day ferrets from the FCC: FCC11283, FCC 8934, FCC8932, and FCC8215.

Genomic libraries were prepared using the Illumina TruSeq DNA PCR-Free Library Prep Kit according to the manufacturer's protocol. Libraries were sequenced on an Illumina NovaSeq X Plus platform using the 10B or 25B flow cell configuration. Sequencing generated paired-end reads of 150 bp in length, with approximately 50 Gb of sequence data produced per sample. The six samples sequenced in the 2nd batch were sequenced at 75G throughput.

2.3 Pre-processing and Alignment

All bioinformatic analyses were performed on the Alpine high performance computing resource at the University of Colorado Boulder. Alpine is jointly funded by the University of Colorado Boulder, the University of Colorado Anschutz, Colorado State University, and the National Science Foundation (Award 2201538; University of Colorado Boulder Research Computing

2023). Additional analyses were done in program R v. 4.4.1 (R Core Team 2024) also through Alpine. Data was visualized with the ggplot2 package (Wickham 2016) in R.

The chromosome-level reference genome for *Mustela nigripes* was obtained from the National Center for Biotechnology Information RefSeq assembly MUSNIG.SB6536 (accession GCF_022355385.1). Chromosome-level scaffolds comprise 2.39 Gbp, representing 95.6% of the assembled genome (Kliver et al. 2023). The assembly additionally contains 20,555 unplaced scaffolds and includes the mitochondrial genome (NC_024942.1). The reference was created from a ferret named Capone, SB# 6536, born in 2009 at the Smithsonian's National Zoo and Conservation Biology Institute (SNZCBI). Capone's dam was a female from the captive breeding program at the time, but his sire was SB# 18 (Scarface), one of our samples, made possible by using Scarface's cryopreserved semen for artificial insemination. This direct relationship between the reference Capone and his father Scarface likely introduced reference bias in many of our downstream analyses.

File integrity of data after download was checked with md5sum hashes provided by Psomagen. Adapter trimming and initial quality filtering was performed with fastp v. 0.23.4 (Chen 2025). Additional quality control on raw and trimmed files was performed with FastQC v. 0.11.9 (Andrews 2010). Reports were aggregated and visualized with MultiQC v. 1.14 (Ewels et al. 2016).

Sequencing depth was consistent across samples and correlated with the two sequencing batches of 20x and 30x depth (Figure 2-1). One outlier from the first 20x sequencing batch was

MSB127011 (SB# 25), which also had the largest raw fastq files (20.9 and 21.2GB) compared to the other 17 samples (range: 12.0 – 16.2GB) and was closer to the 30x batch file size (17.0-21.2GB). Sequencing quality was high across all samples, with mean Phred scores per sequence exceeding Q30.

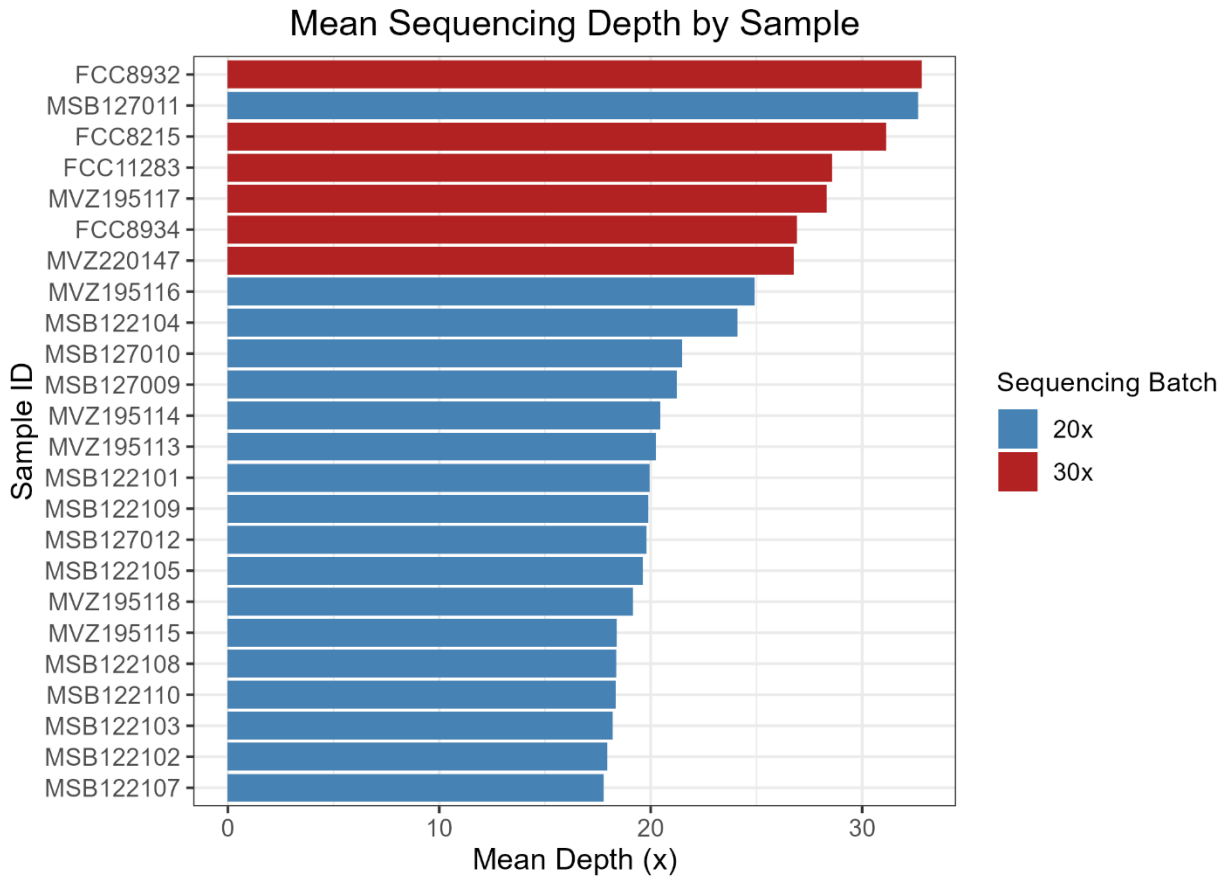

Figure 2-1. Mean sequencing depth across the two sample batches of 20x and 30x depth.

Trimmed fastq files were aligned to the reference genome using BWA-MEM2 v.2.2.1 (Vasimuddin et al. 2019). Mapping success to the reference was greater than 99% across all samples (Figure 2-2).

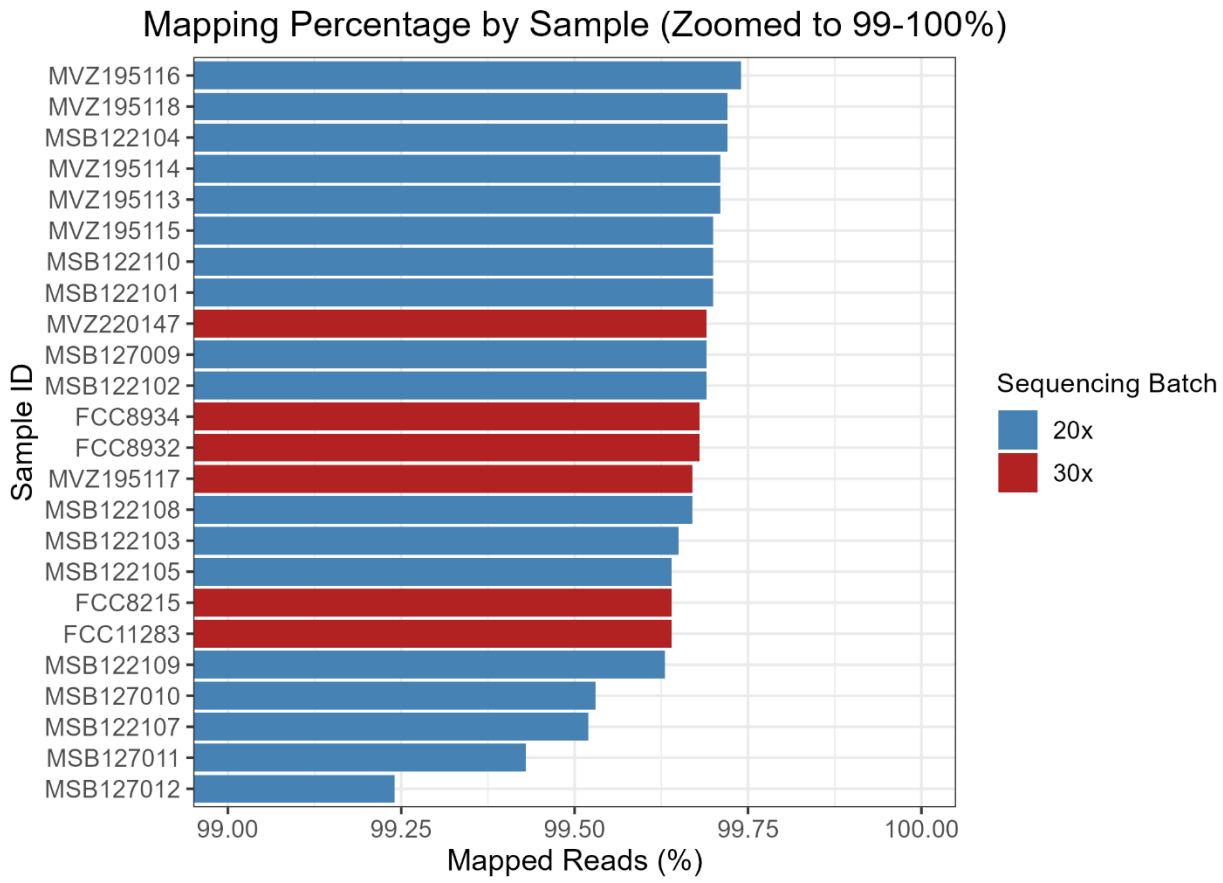

Figure 2-2. Percent of mapped reads by sample. All samples were mapped above 99%.

Resulting SAM files were compressed to BAM format with samtools v. 1.16.1 (Danecek et al. 2021). BAM file processing, including collating, sorting, indexing, and duplicate marking, was handled with samtools v. 1.16.1 (Danecek et al. 2021). We set the optical distance flag at 2500 to optimize marking for NovaSeq platforms, per samtools documentation. We compared optical duplicate rates among sequencing flowcells using a Kruskal–Wallis rank-sum test in R. Mapping QC was performed with stats files from samtools' flagstat and stats output and then visualized with MulitQC. Duplicate read rate clustered strongly by flowcell (Kruskal–Wallis test: $\chi^2 = 21.52$, df = 4, $p = 0.00025$; Figure 2-3). This aligns with the expected optical duplicate behavior from Illumina NovaSeq X patterned flowcells and a PCR-free library prep.

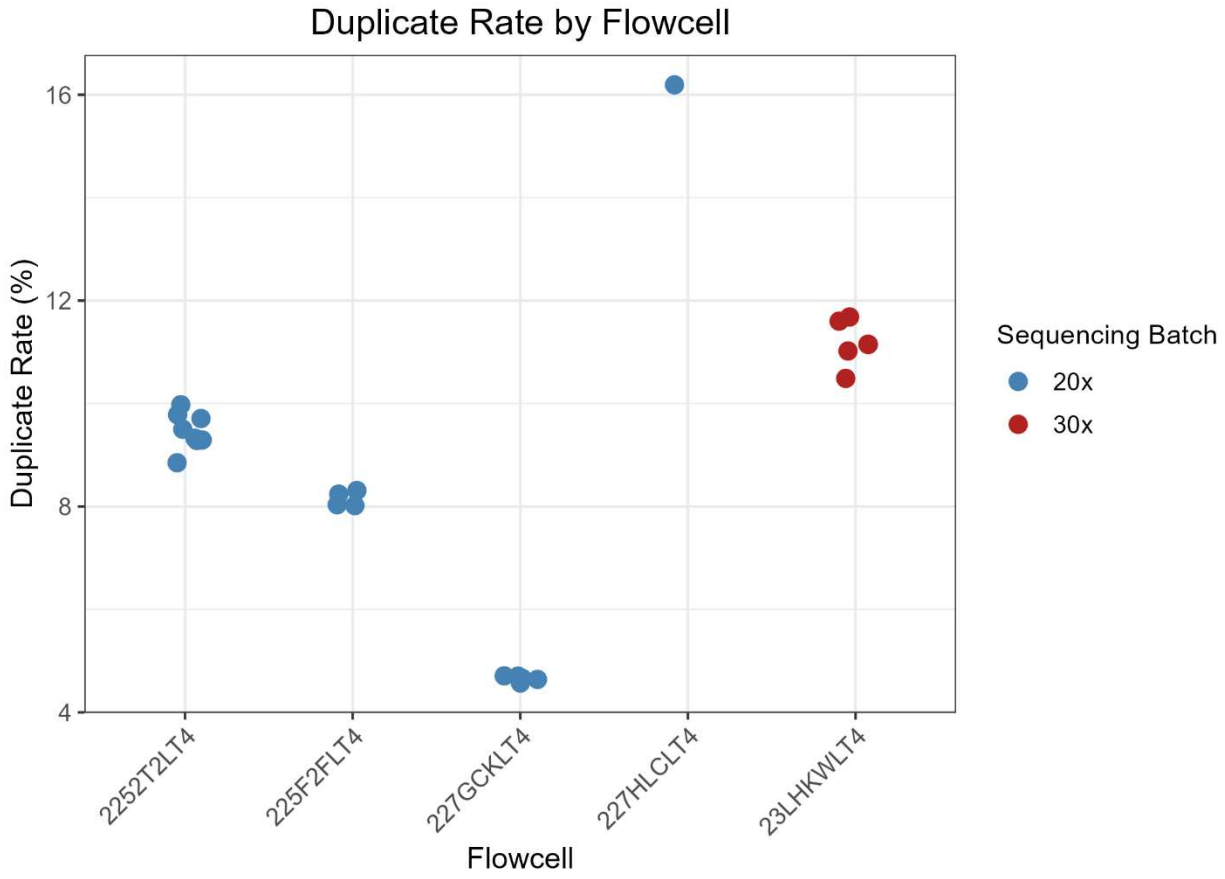

Figure 2-3. Optical duplicate read rate by flowcell, colored by sequencing batch.

2.4 Variant Depth and Filtration

We followed a bioinformatic pipeline based on the Genome Analysis Toolkit (GATK) best practices for variant discovery but adapted for the black-footed ferret as a non-model species. Note that we did not perform Base Quality Score Recalibration (BQSR) as no datasets of known variants are readily available for the black-footed ferret. Genomic Variant Call Format (GVCF) files were produced for each sample with the GATK4 v. 4.5.0 (Van der Auwera and O'Connor 2020) tool HaplotypeCaller. We performed joint genotyping using GenomicsDBImport and GenotypeGVCFs (Poplin et al. 2018). To restrict downstream analyses to well-resolved regions

of the genome, variant calling was limited to the 19 assembled chromosomes of the reference genome (the 18 autosomes and the X chromosome). Unplaced and unlocalized contigs were excluded from the analysis using an interval list corresponding to the chromosome-level scaffolds. To improve efficiency and run time, we parallelized GenotypeGVCFs over the 19 chromosomal intervals and concatenated the resulting Variant Call Format (VCF) files with BCFtools v. 1.23 (Danecek et al. 2021).

All individuals were included in the variant call set to reduce ascertainment bias, with VCF files subsetted downstream as needed for specific analyses. Variants were first restricted to biallelic SNPs using GATK4 SelectVariants. Because insufficient training data and truth sets exist for the non-model black-footed ferret to support Variant Quality Score Recalibration (VQSR), hard filtering was performed using GATK4 VariantFiltration. Standard GATK hard filters were applied using the following thresholds: QD < 2.0, QUAL < 30.0, SOR > 3.0, FS > 60.0, MQ < 40.0, MQRankSum < -12.5, and ReadPosRankSum < -8.0. The number of variants of the initial 1,214,251 biallelic SNPs flagged by each filter is shown in Figure 2-4. The SOR > 3.0 filter failed more variants than any other, and the distribution of SOR values is shown in Figure 2-5.

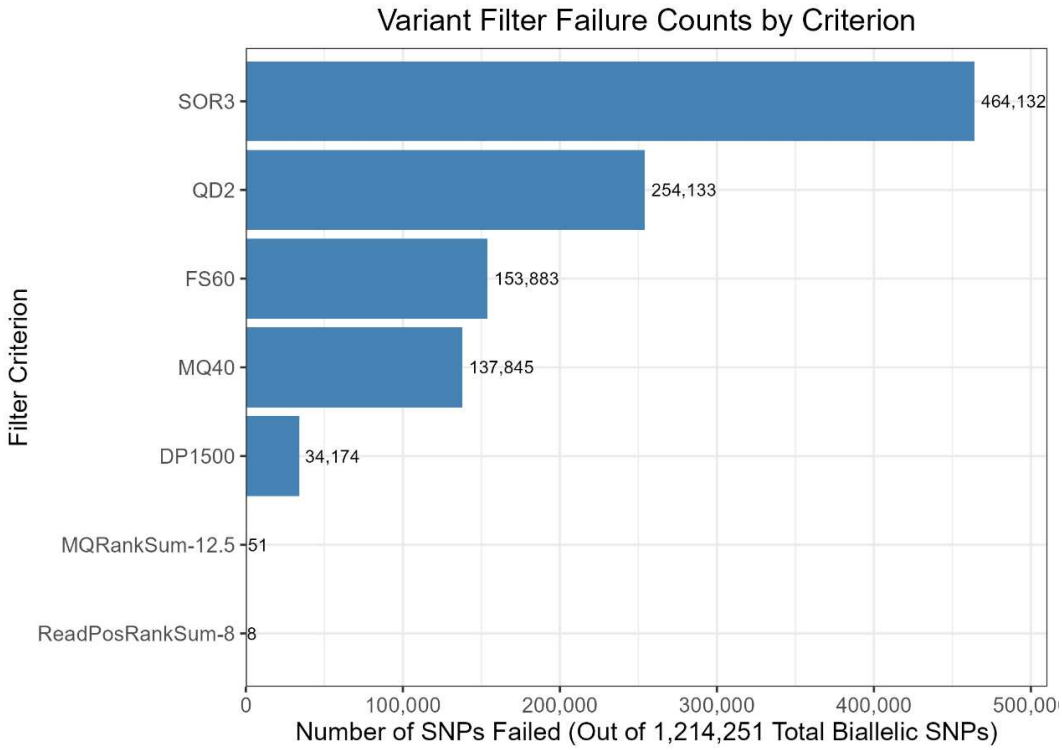

Figure 2-4. Number of variants flagged by each hard filter in GATK. Note that sites can fail multiple filters.

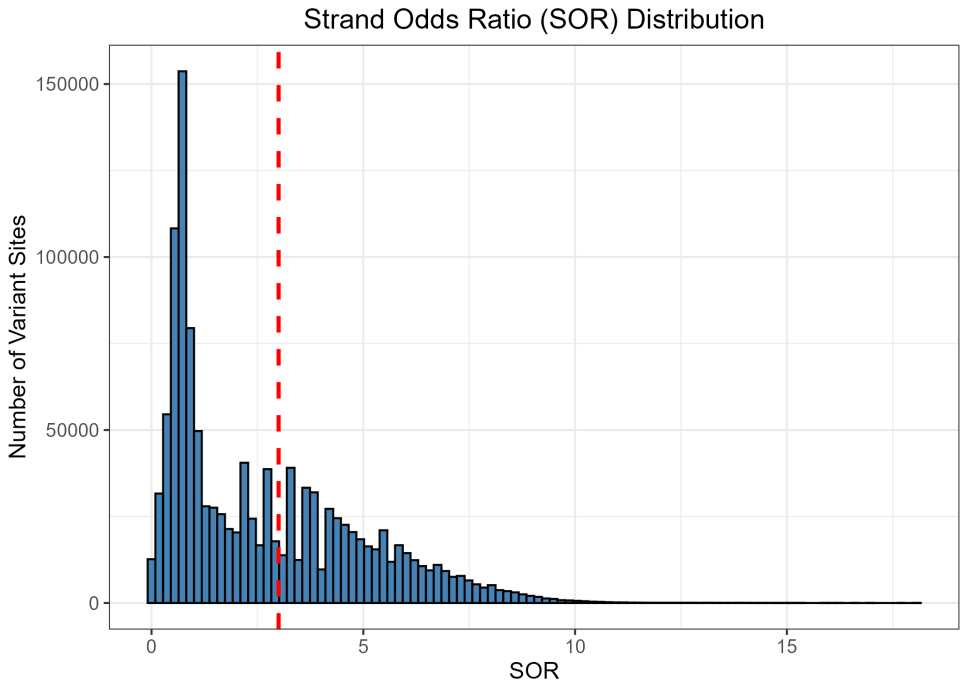

Figure 2-5. Distribution of SOR values among raw biallelic SNPs. Red dashed line indicates the filter threshold of 3.0.

An additional site-level depth filter of INFO/DP > 1500 was applied to remove variants with unusually high coverage. Extremely high-depth variant calls are frequently associated with mapping artifacts, collapsed repeats, or low-complexity regions and may appear falsely confident because of excessive read support. Mean site depth across biallelic SNPs in the raw VCF was 582.3×, consistent with expectations based on sequencing depth and sample number (Figure 2-6). However, the distribution of site depth exhibited a heavily right-skewed tail extending beyond 100,000× depth (Figure 2-6). The samtools/HTSlib VCF filtering guidelines note that genuine variant calls are often absent at sites with coverage substantially exceeding the expected mean depth. Therefore, variants with INFO/DP > 1500 (approximately three times the mean site depth) were removed from downstream analyses.

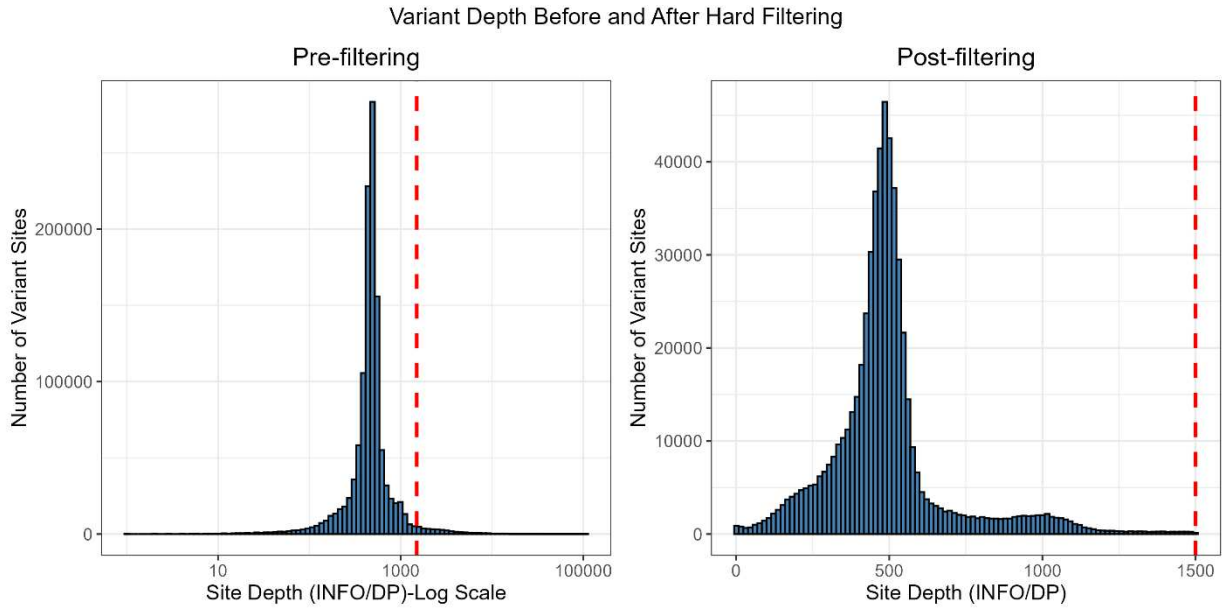

Figure 2-6. Variant depth before and after applying hard filters. Pre-filtering panel is shown with the x-axis on the log scale. Red dashed line indicates filter threshold.

Genotype-level filtering was performed using values from the FORMAT field of the VCF. Genotype depth (FORMAT/DP) exhibited a strongly right-skewed distribution extending to

nearly 10,000× coverage; application of site-level hard filters substantially reduced this tail (Figure 2-7). Genotype quality (FORMAT/GQ) distributions also shifted following application of hard filters, with a reduction in the proportion of low-confidence genotype calls (Figure 2-8).

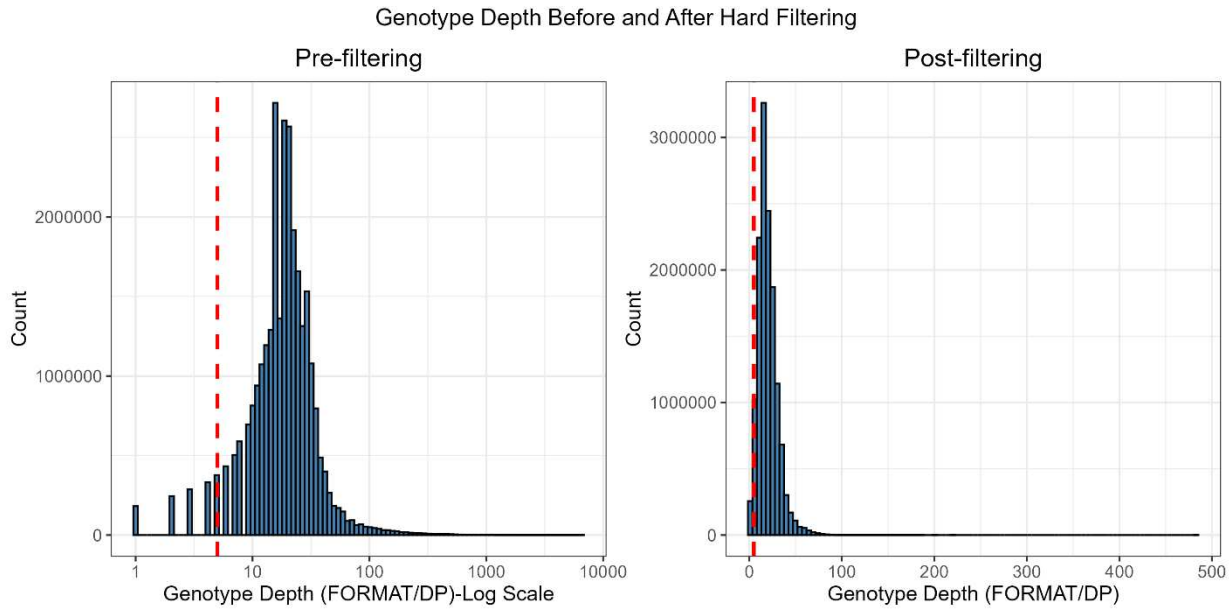

Figure 2-7. Distribution of genotype depth before and after hard filters. Pre-filtering panel is shown with the x-axis on the log scale. Red dashed line indicates the anticipated GP filter threshold of 5.

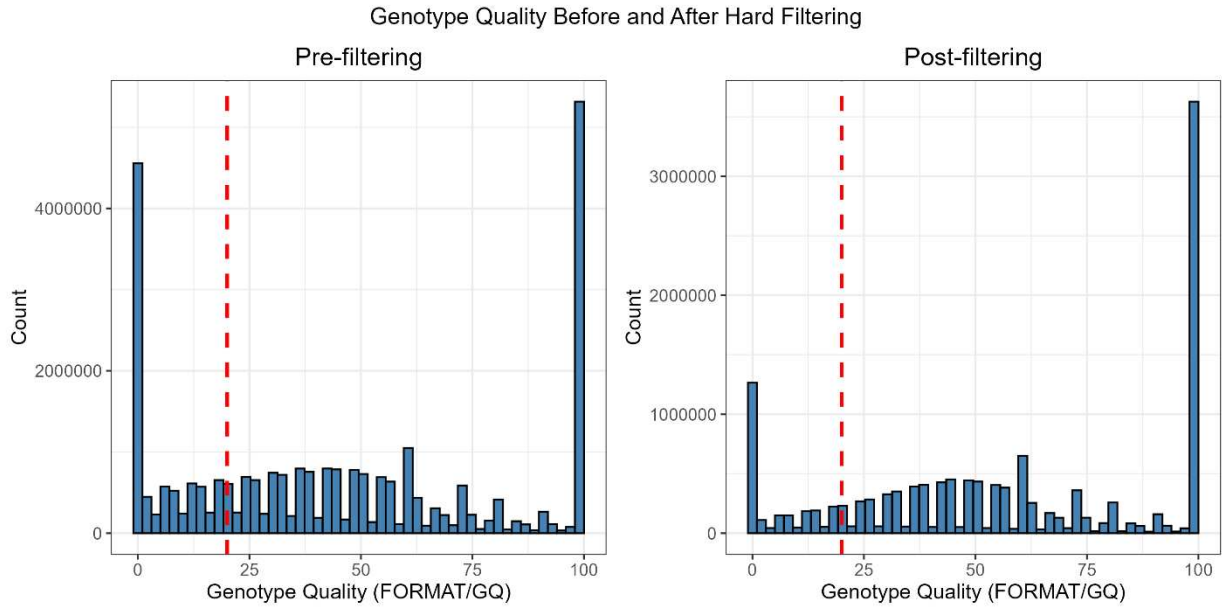

Figure 2-8. Genotype quality of biallelic SNPs before and after hard filters. Red dashed line indicates the anticipated GQ filter threshold of 20.

To remove poorly supported genotype calls, genotypes with depth < 5 reads were flagged using the GATK genotype filter DP < 5. Additional genotype-level filtering was performed using genotype quality (GQ), a Phred-scaled confidence metric representing the difference between the most likely and second most likely genotype calls. Genotypes with GQ < 20 were flagged as low confidence. A GQ threshold of 20 corresponds to an estimated error probability of approximately 1%. Song et al. (2016) reported that combined genotype filters of DP < 5 and GQ < 20 produced >95% genotype accuracy.

2.5 Missingness

Prior to genotype-level filtering, missingness across the dataset was minimal. Missing genotype calls in the site-filtered VCF ranged from approximately 0.03–0.05% among individuals in the 20× sequencing batch and approximately 0.01% in the 30× sequencing batch. Across callable sites, 99.45% had complete genotype calls for all individuals. Missingness increased

substantially following genotype depth and quality filtering, which masked unreliable and low-depth genotype calls. Flagged genotypes from these filters were converted to missing calls (./.) for downstream analyses. Individual missingness increased to approximately 15–21% in the 20× sequencing batch and 11–13% in the 30× sequencing batch (Figure 2-9). Following genotype filtering, sites with complete genotype calls across all individuals decreased to 45.02% of callable sites. Because of this additional missing data, downstream analyses incorporating genotype filters were also filtered for missingness. In some cases, genotype filtering converted previously variable sites into invariant sites when all alternate genotype calls were removed; these invariant sites were subsequently excluded where appropriate. Missingness statistics were calculated using VCFtools v0.1.17 (Danecek et al. 2011).

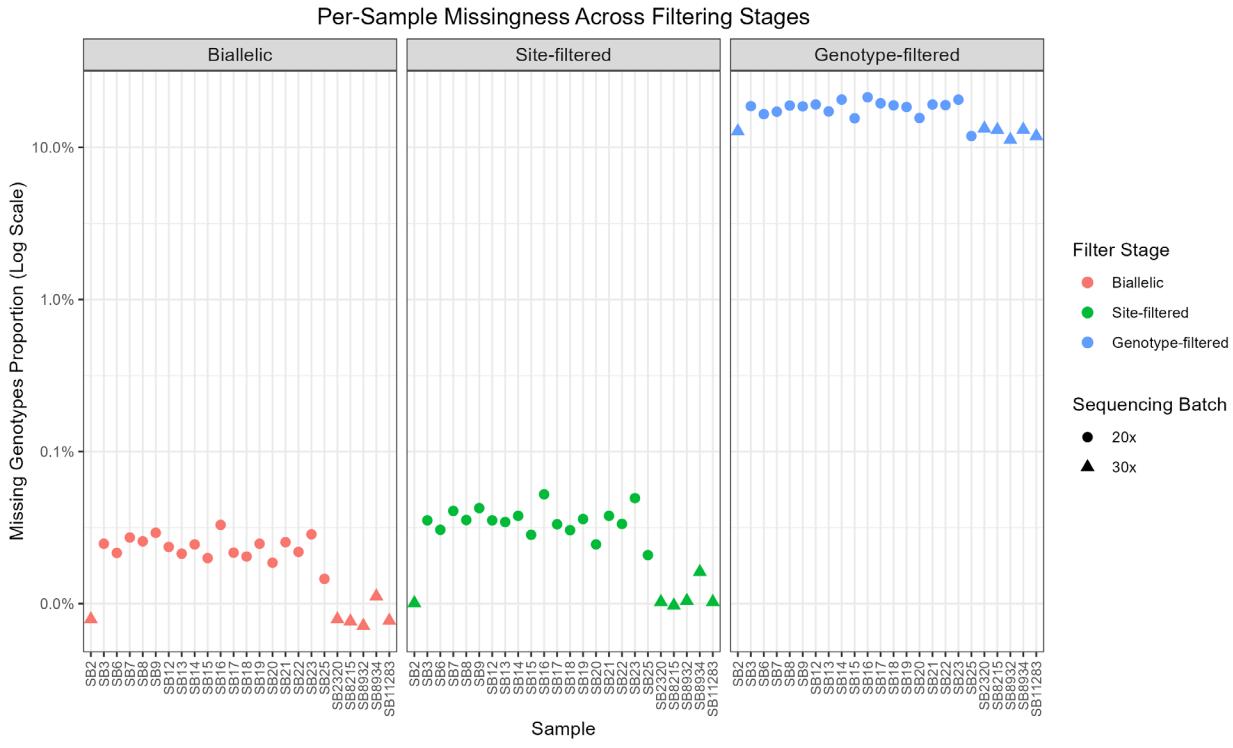

Figure 2-9. Per-sample missingness across filtering stages, shown on the log scale.

Application of genotype depth and quality filters also introduced a noticeable heterozygote excess. This excess was substantially reduced after filtering sites with >10% missing data (Figure 2-10). All downstream analyses conducted after genotype-level filtering incorporated additional missingness thresholds appropriate to the specific analysis.

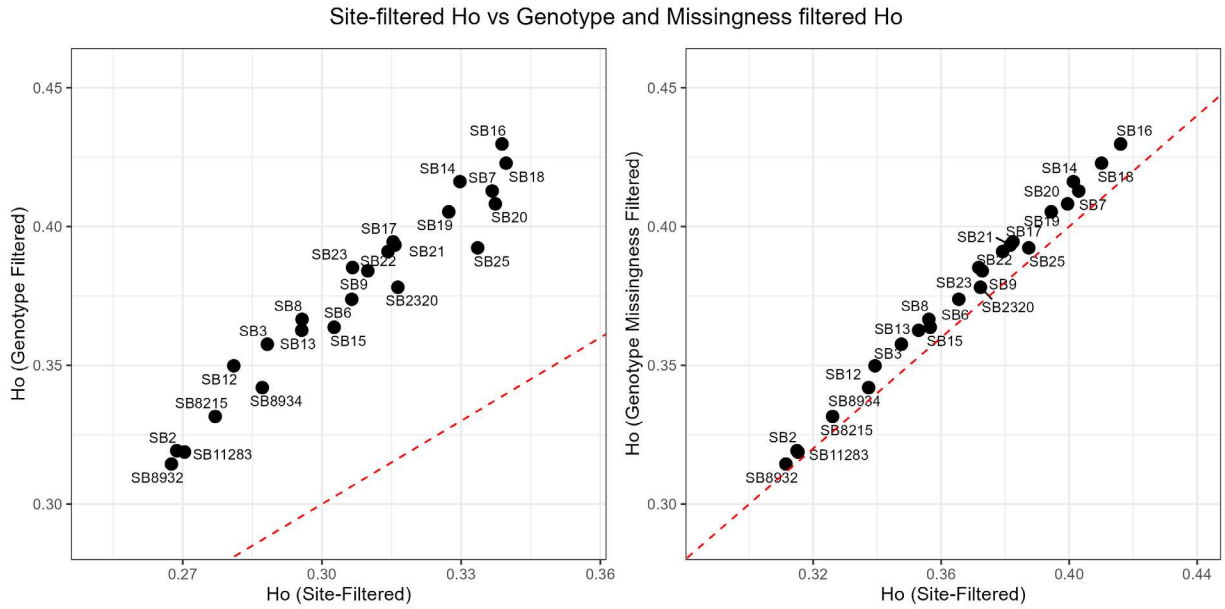

Figure 2-10. Observed heterozygosity among called variants in the site-filtered VCF compared to the genotype filtered VCF, before and after filtering for missingness >10%/site

2.6 Downstream Analyses

2.6.1 Genome-wide Heterozygosity

The folded site frequency spectrum (SFS), which summarizes the distribution of minor allele frequencies without requiring knowledge of ancestral allele states, and genome-wide heterozygosity were estimated from BAM files for each sample across the 18 autosomal chromosomes using ANGSD v.0.940 (Korneliussen et al. 2014). The reference genome was supplied for the -anc argument (required by ANGSD); however, because no ancestral genome exists for black-footed ferrets, the folded SFS (-fold) was used with the downstream realSFS

command. ANGSD filtered sites prior to analysis for mapping quality (-minMapQ 30), base quality (-minQ 20), depth (-setMinDepthInd 5, -setMaxDepthInd 60), and adjusted for alignment quality/mismatches (-baq 1, -C 50). We used the Samtools genotype likelihood model (-GL 1). We used reported number of callable sites to estimate genome size per individual. We used windowed thetaPi (nucleotide diversity) every 50kb as a measure of heterozygosity across the autosomal genome. We used a Wilcoxon rank-sum test to assess differences in heterozygosity between founder and descendant populations. We assessed observed heterozygosity of site-filtered and genotype-filtered VCFs with VCFtools v 0.1.17 (Danecek et al. 2011).

2.6.2 Runs of Homozygosity

To characterize genome-wide runs of homozygosity (ROH), or contiguous lengths of chromosomal regions that contain no heterozygous nucleotide sites, we used the BCFtools hidden Markov model approach (Narasimhan et al. 2016) with the site-and genotype-filtered VCF filtered for missingness for all 24 samples and restricted to just the 18 autosomal chromosomes. We estimated the inbreeding coefficient based on the summed lengths of homozygous regions, F_{ROH}, as the proportion of the total autosomal genome length contained within ROH (Allendorf et al. 2022). Autosomal genome length was estimated from the reported lengths for black-footed autosomal chromosomes in the reference genome (Kliver et al. 2023). We used a Wilcoxon rank-sum test to assess differences in F_{ROH} between source and descendant populations.

2.6.3 PCA and Kinship

We utilized the site and genotype-filtered 19-chromosome VCF to assess relatedness and to inform principal component analysis (PCA). We used PLINK 2 v. 2.00a2.3. (Chang et al. 2015) to prune the VCF for linkage disequilibrium (LD) using a sliding window approach (window size 50, step size 10, LD threshold 0.1) to produce a set of independent SNPs, and to filter for minor allele frequency (MAF 0.05) and site missingness greater than 10% (geno 0.1). For some plots and the relatedness matrix we did not use a MAF filter to visualize rarer variation. We used the PLINK2 –pca command to output eigenvectors and eigenvalues for PCA visualization in R. We estimated kinship (ϕ) between individuals with pairwise kinship coefficients using the PLINK2 KING-robust estimator derived from Manichaikul et al. (2010). To evaluate the relationship between the reported pedigree and genomic estimates of relatedness, we fit a linear-mixed effects model (lmer(GEN_KINSHIP ~ EXP_KINSHIP + (1 | ID1) + (1 | ID2)) with the R package lme4 (Bates et al. 2015), with genomic kinship as the response variable and expected pedigree kinship as a fixed effect. Since individuals appeared multiple times in pairwise comparisons, we included random variables for both individual IDs to account for this pseudo-replication. Differences between expected pedigree kinship and observed genomic kinship were compared between first-degree pairs and assumed unrelated pairs using a Wilcoxon rank-sum test based on absolute kinship deviations in R.

2.6.4 Pedigree Hypothesis Testing and Inference

We tested the likelihood of the expected relationships from the initial assumed pedigree (Figure 1-3) and inferred relationships from the genomic data using the R package Sequoia v. 3.2.0 (Huisman 2017). We filtered an appropriately sized panel of maximally informative and high-

confidence SNPs with minimal error from the site- and genotype-filtered autosomal VCF of the 19 wild-captured individuals. We applied a maximum missingness filter of 0.95 (max missing allowed = 0.05) and a minor allele frequency filter of 0.5 with VCFtools. Lastly, we pruned for linkage disequilibrium (LD) with PLINK2 with a tightened indep-pairwise 50 5 0.1.

To reconstruct a pedigree from the resulting SNPs, we used the sequoia function. We used CalcOHLLR in Sequoia v. 3.2.0 to compare the assumed input pedigree to an inferred pedigree from the filtered SNP data. This tests parent-offspring relationships via log likelihood ratios and counts how many SNPs are consistent with the parent-offspring genotypes. We used GetMaybeRel in Sequoia to look for other potential close relationships.

2.6.5 Retained Variation and Private Alleles

To assess retention of genetic variation from the Meeteetse source population, we used the R packages vcfR (Knaus and Grünwald 2017) and tidyverse (Wickham et al. 2019) to analyze the autosomal site- and genotype-filtered VCF. Variant sites were defined relative to the reference genome, where the reference allele (REF) matched the reference assembly and alternate alleles (ALT) represented observed sequence variation. To minimize erroneous inference of allele frequencies within the source population, sites containing missing genotypes in any source-population individual were excluded, as missing data could mask ALT allele calls. For each variant site, ALT allele frequencies were calculated across source-population individuals and compared to frequencies observed in descendant individuals. Source-population polymorphisms were classified according to their evolutionary fate in descendant populations as retained polymorphism, ALT allele loss, or ALT allele fixation.

Founder-private alleles were analyzed separately as loci where only a single genetic founder carried the ALT allele, either in heterozygous or homozygous form. Using the same source-population complete filtered dataset, we identified founder-private variants and quantified their persistence in descendant generations by determining whether the ALT allele remained present in at least one descendant individual. These analyses were used to evaluate lineage-specific retention of unique variation through the bottlenecked founder population.

CHAPTER 3: RESULTS

3.1 Variant Calling

Variant calling identified 1,611,545 candidate variants across all 24 individuals, including 1,255,070 SNPs and 366,266 insertions/deletions (indels). For our analyses we kept only SNPs. Table 3.1 shows changing SNP counts with various stages of variant filtration and VCF subset. The raw 24-sample dataset exhibited a transition/transversion (Ts/Tv) ratio of 1.31. Ts/Tv ratio improved only slightly with hard filtering to 1.33 but improved moderately to 1.57 after removing sites with greater than 10% missing genotypes introduced by the genotype filters. In general, transitions (substitutions within the same nucleotide class, purines or pyrimidines) are more common than transversions (substitutions between purines and pyrimidines) in mammalian genomes but can vary among species (Belle et al. 2005; Allendorf et al. 2022).

Table 3.1. SNP count and Ts/Tv ratio by filtering step

Stage	**File (.vcf.gz)**	**SNPs**	**Ts/Tv ratio**
Raw VCF	founders_24	1,255,070	1.31
Biallelic	founders_24_snp_biallelic	1,214,251	1.34
Hard filters	founders_24_sitefiltered	574,417	1.33
Genotype filters	founders24_gq20	565,141	1.34
Missingness filtered (> 10%/site)	founders24_gq20_geno01	355,999	1.57
Source population subset	founders19_gq20	555,276	1.34
Missingness filtered (> 10%/site)	founders19_gq20_geno01	325,268	1.61

3.2 Genome-wide Heterozygosity

ANGSD evaluated approximately 2.21 billion sites per individual. After filtering, approximately 2.19 billion sites per individual were retained for analysis, which was consistent across samples (2.189 to 2.199 billion sites retained). Autosomal genome-wide heterozygosity across samples is reported in Table 3.2.

Table 3.2. Heterozygosity across the autosomal genome with estimated number of bp per SNP

Sample	SB_No	Callable_Genome_Gb	Heterozygosity	BP_per_SNP
MVZ195117	2	2.199	0.00002847	35121
MVZ195118	3	2.190	0.00002724	36709
MSB127009	6	2.196	0.00003178	31469
MVZ195114	7	2.195	0.00003446	29022
MVZ195115	8	2.191	0.00002910	34361
MVZ195113	9	2.196	0.00003267	30605
MSB122103	12	2.192	0.00002802	35691
MSB127010	13	2.196	0.00003006	33269
MSB122107	14	2.192	0.00003382	29566
MVZ195116	15	2.197	0.00003061	32665
MSB127012	16	2.192	0.00003599	27782
MSB122108	17	2.192	0.00003266	30614
MSB122109	18	2.195	0.00003621	27617
MSB122105	19	2.194	0.00003425	29201
MSB122104	20	2.197	0.00003450	28983
MSB122101	21	2.194	0.00003216	31098
MSB122110	22	2.193	0.00003253	30738
MSB122102	23	2.191	0.00003067	32601
MSB127011	25	2.198	0.00003321	30110
MVZ220147	2320	2.197	0.00003382	29568
FCC8215	8215	2.192	0.00002838	35239
FCC8932	8932	2.199	0.00002822	35434
FCC8934	8934	2.199	0.00003158	31669
FCC11283	11283	2.199	0.00002871	34827

Heterozygosity ranged from 0.00002724 to 0.00003621 (mean = 0.00003203) in the Meeteetse source population and from 0.00002822 to 0.00003382 (mean = 0.00003014) in the descendant subset (Figure 3-1). Genome-wide heterozygosity was lower in the five descendant ferrets than in the source individuals, although this difference was not statistically significant (Wilcoxon

rank-sum test: W = 27, p = 0.16). The intermediate animal SB# 2320 born in 1998 is a high outlier for the descendant population with heterozygosity 0.00003382, above the mean for the source population animals. Excluding him from the descendant group (mean = 0.00002922) strengthened the trend but did not reach significance (Wilcoxon rank-sum test: W = 14, p = 0.054).

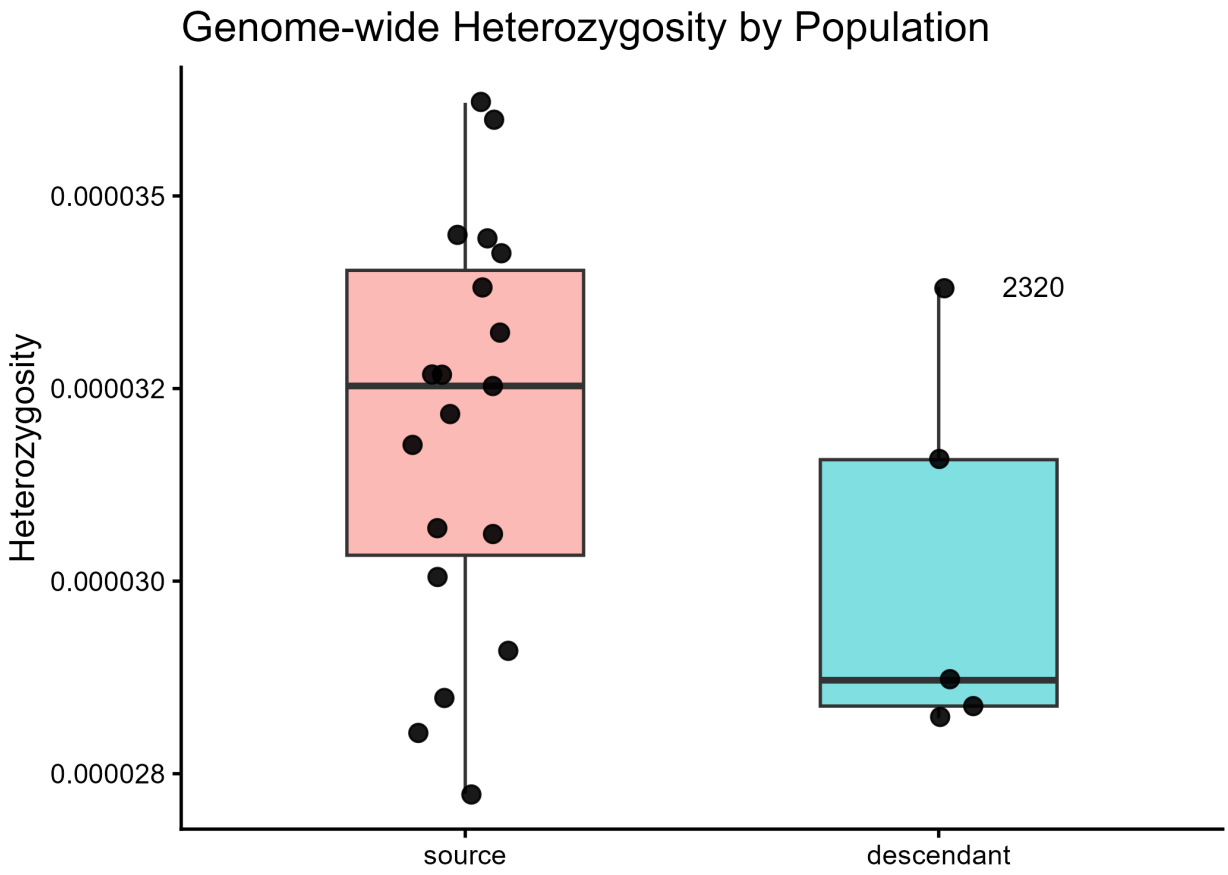

Figure 3-1. Genome-wide heterozygosity by founder and descendant populations. The intermediate descendant SB2320 is labeled.

Mean genome-wide heterozygosity in source and descendant black-footed ferrets is shown in Figure 3-2. Distributions of heterozygosity across 50 kb genomic windows are shown in Figure

3-3.

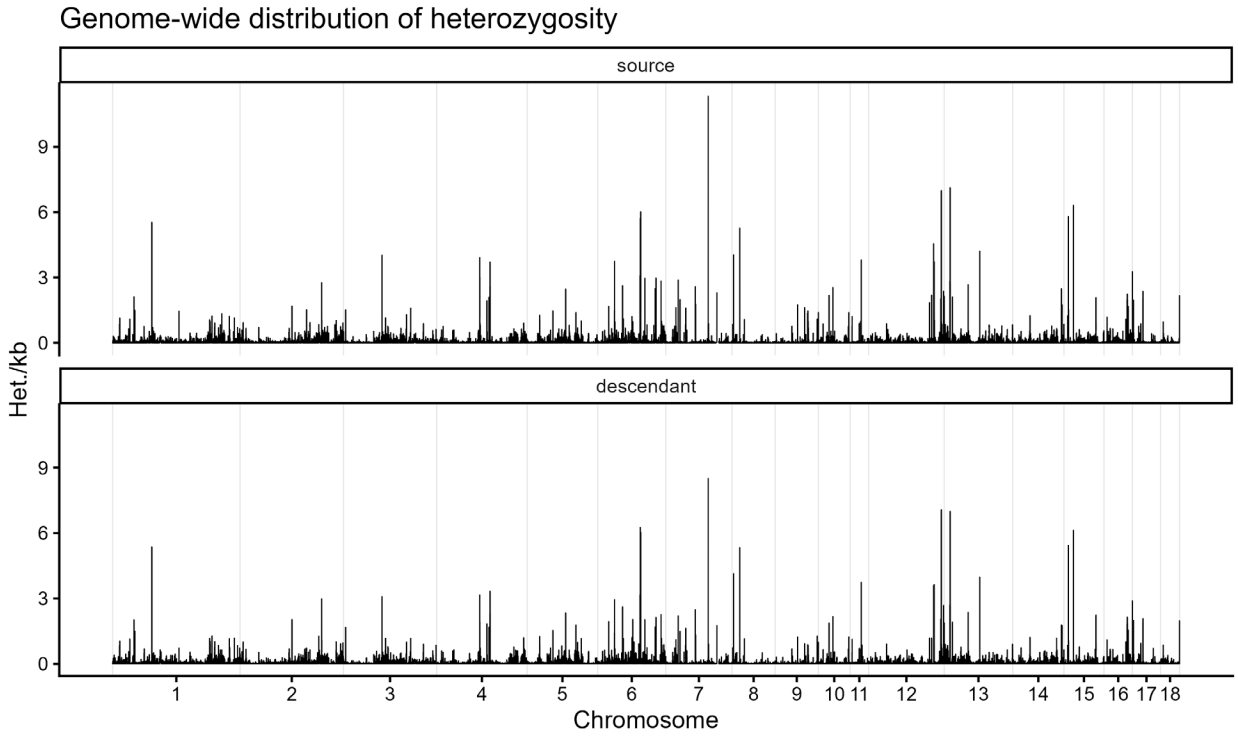

Figure 3-2. Mean estimated heterozygosity across the genome in source population and descendants. Heterozygosity is shown in heterozygous sites per Kb (1000 bases) across the 18 autosomal chromosomes.

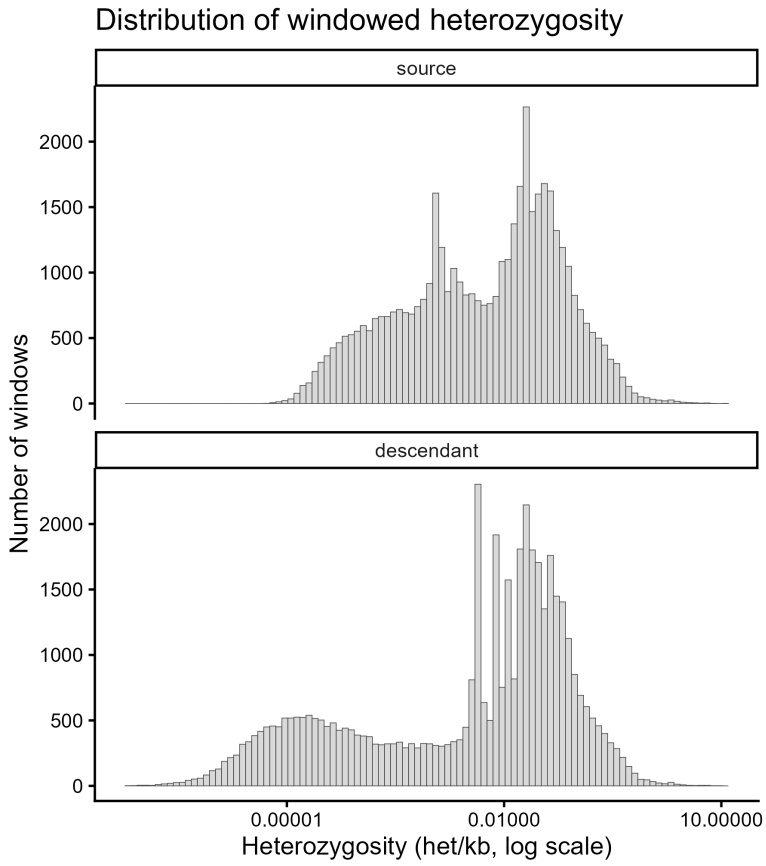

Figure 3-3. Frequency distribution of mean windowed heterozygosity estimates for each population on a log-scaled x-axis.

Windowed nucleotide diversity across the 18 autosomal chromosomes in 50kb windows for all samples is shown in Figure 3-4, Figure 3-5, and Figure 3-6. Collectively these plots highlight patterns of heterozygosity across the autosomal black-footed ferret genome. Visual inspection reveals that some chromosomes (e.g., chromosomes 8 and 9) are especially depauperate of nucleotide diversity. Most areas of heterozygosity seem to be shared between at least two individuals with the exception of SB# 16 (Dean), who occasionally displays heterozygous areas unique to his sample (note chromosomes 7 and 8).

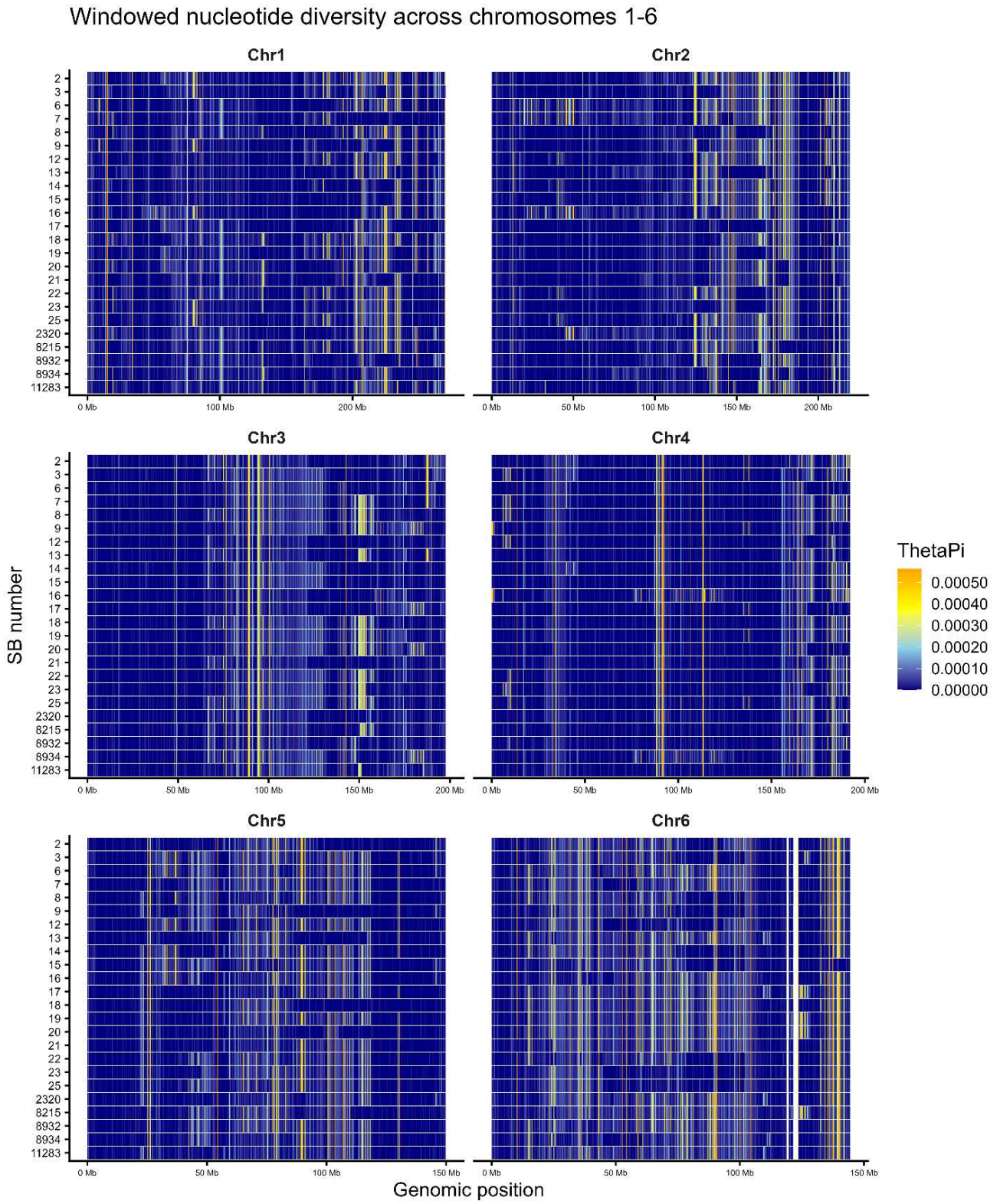

Figure 3-4. Windowed nucleotide diversity across autosomal chromosomes 1 -6 among the 19 source and five descendant individuals. Sliding window size = 50kb. Warmer colors indicate genomic areas of higher SNP density; areas of chromosomes that are entirely blue are homozygous.

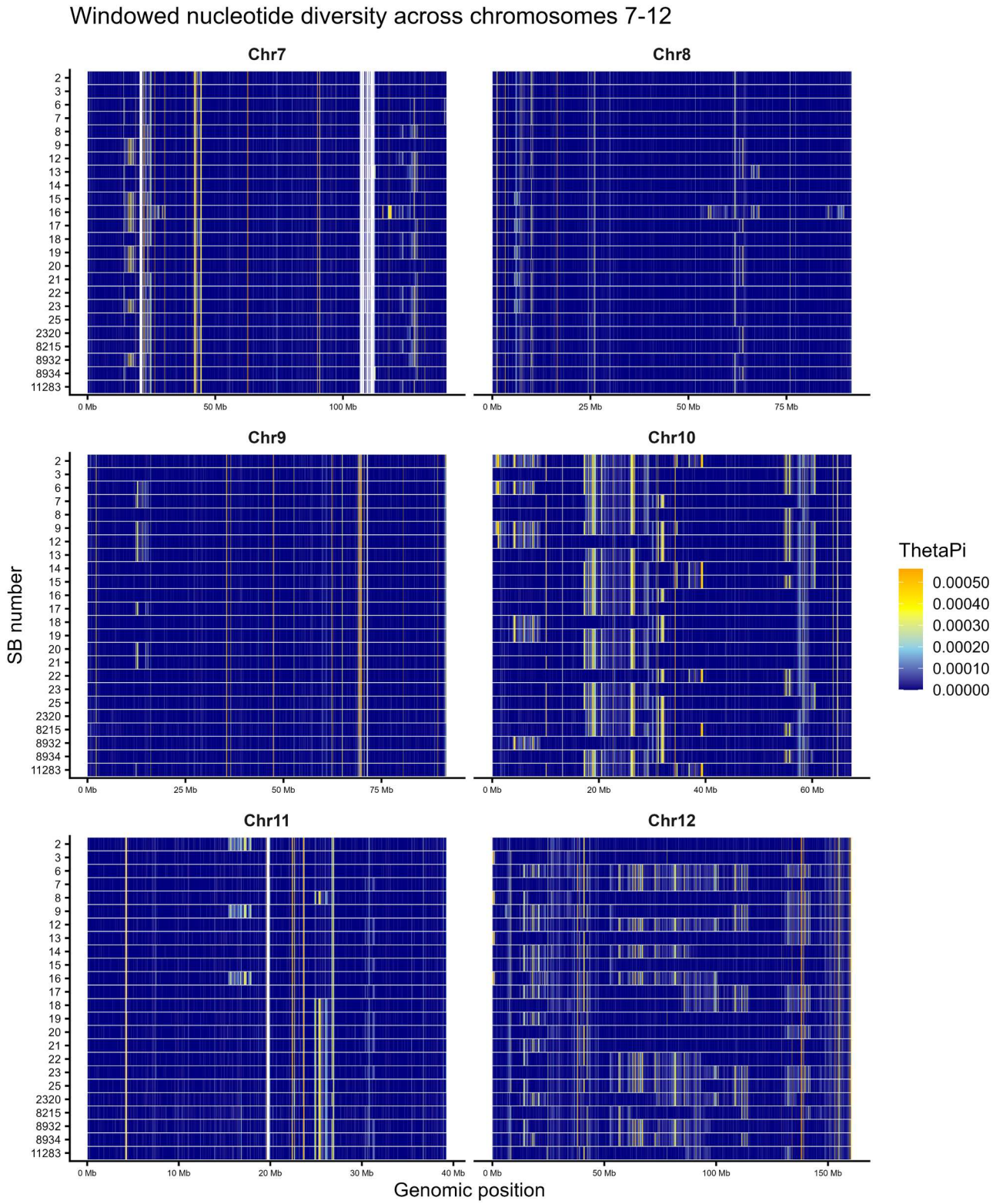

Figure 3-5.Windowed nucleotide diversity across autosomal chromosomes 7-12 among the 19 source and five descendant individuals. Sliding window every size = 50kb. Warmer colors indicate genomic areas of higher SNP density; areas of chromosomes that are entirely blue are homozygous.

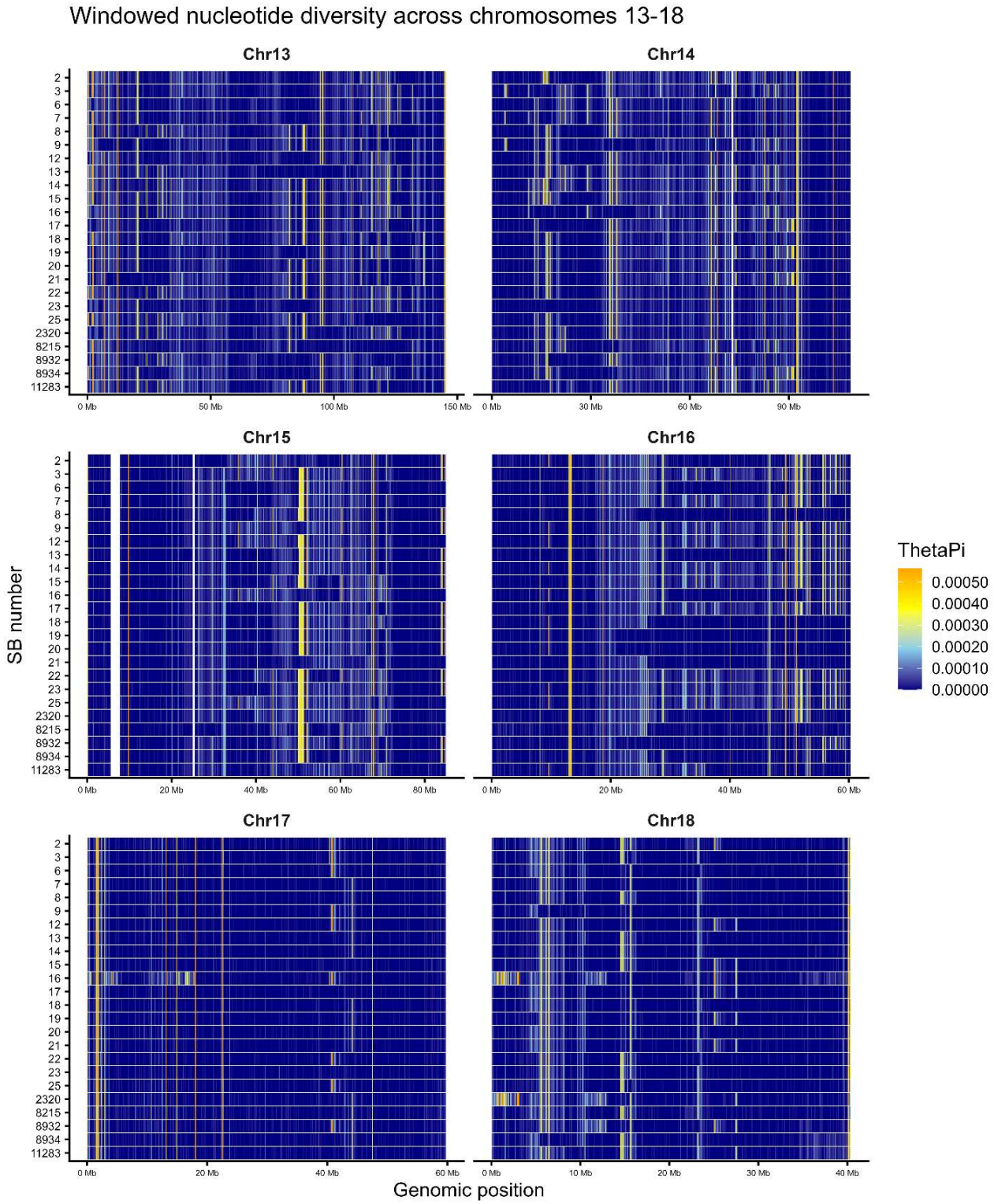

Figure 3-6. Windowed nucleotide diversity across autosomal chromosomes 13-18 among the 19 source and five descendant individuals. Sliding window size = 50kb. Warmer colors indicate genomic areas of higher SNP density; areas of chromosomes that are entirely blue are homozygous.

3.3 Runs of Homozygosity

Total number of runs of homozygosity (ROH) per individual as identified by BCFtools are shown in Table 3.3 along with the total Mb of ROH and the estimated proportion of the genome in ROH (F_{ROH}).

Table 3.3. Summary of ROH number, length, and F_{ROH} in all 24 samples.

Sample	N_ROH	Total_ROH_Mb	F_{ROH}	Sample	N_ROH	Total_ROH_Mb	F_{ROH}
SB2	542	676.4	0.299	SB18	334	385.4	0.170
SB3	660	443.1	0.196	SB19	389	395.1	0.174
SB6	506	511.4	0.226	SB20	435	409.8	0.181
SB7	426	386.0	0.170	SB21	452	384.6	0.170
SB8	502	457.6	0.202	SB22	383	416.6	0.184
SB9	451	503.4	0.222	SB23	486	438.0	0.193
SB12	527	534.8	0.236	SB25	491	465.7	0.206
SB13	472	495.7	0.219	SB2320	463	463.8	0.205
SB14	407	343.6	0.152	SB8215	468	571.1	0.252
SB15	491	503.5	0.222	SB 8932	541	598.3	0.264
SB16	491	389.0	0.172	SB8934	500	543.6	0.240
SB17	373	415.5	0.184	SB11283	560	593.3	0.262

Comparing the source and descendant populations, the descendants had increased homozygosity (mean $F_{ROH\_descendant} = 0.244$, mean $F_{ROH\_source} = 0.199$; Figure 3-7). Interpreted cautiously because of the disparate sample sizes, this increased homozygosity of the descendant ferrets compared to the source ferrets was significant based on a Wilcoxon rank-sum test ($W=11$, $p = 0.0071$). However, the number of ROHs (N_ROH) per individual did not differ significantly between groups (Wilcoxon rank-sum test: $W = 28$, $p = 0.177$).

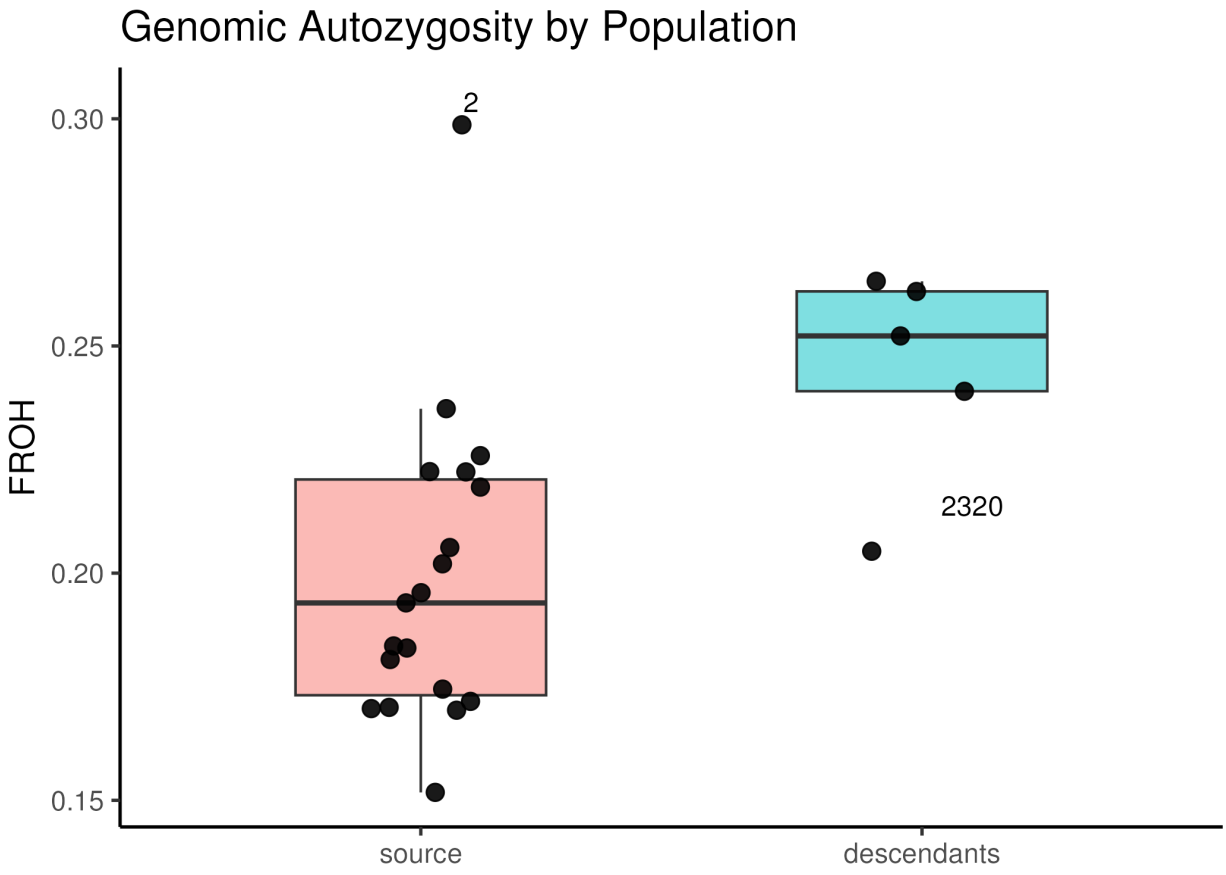

Figure 3-7. Estimated F_{ROH} by source population and descendant groups.

Modern descendants (excluding SB# 2320 from 1998) carried the largest proportions of ROH, along with the outlier from the source population, SB# 2. Mean length of ROHs across all samples was 0.998Mb (SD = 0.851Mb; Figure 3-8). Proportion of ROHs greater than 5Mb in length was relatively small, with no ROH exceeding 10Mb, potentially indicating patterns of historic bottlenecks versus recent inbreeding (Thompson 2013) (Figure 3-9).

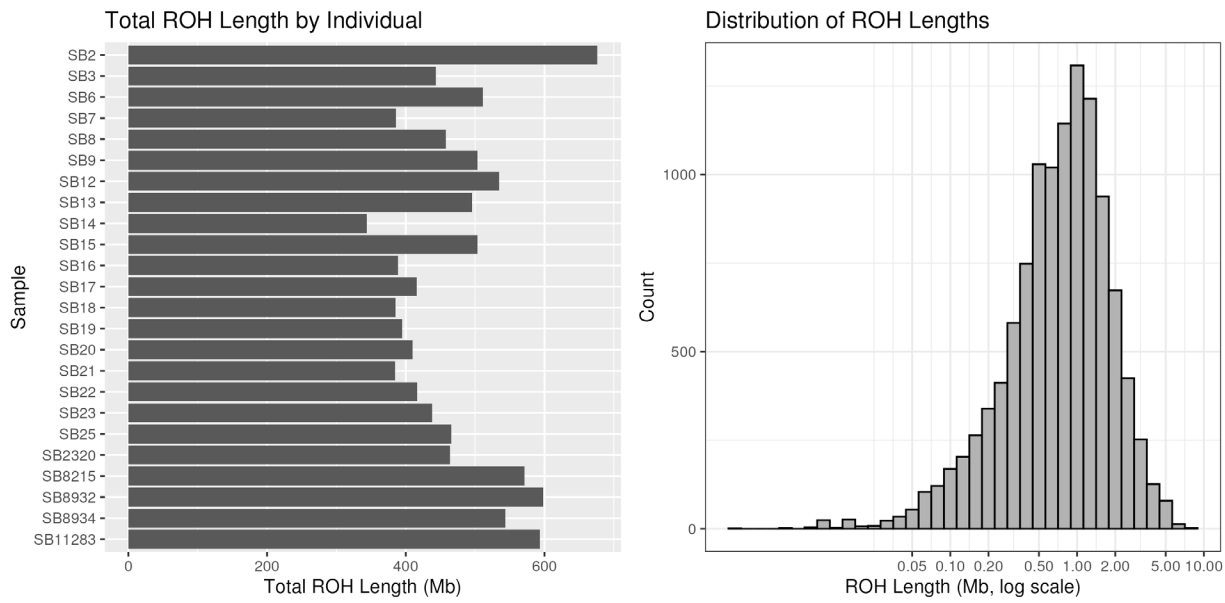

Figure 3-8. Total ROH length by individual and distribution of ROH length.

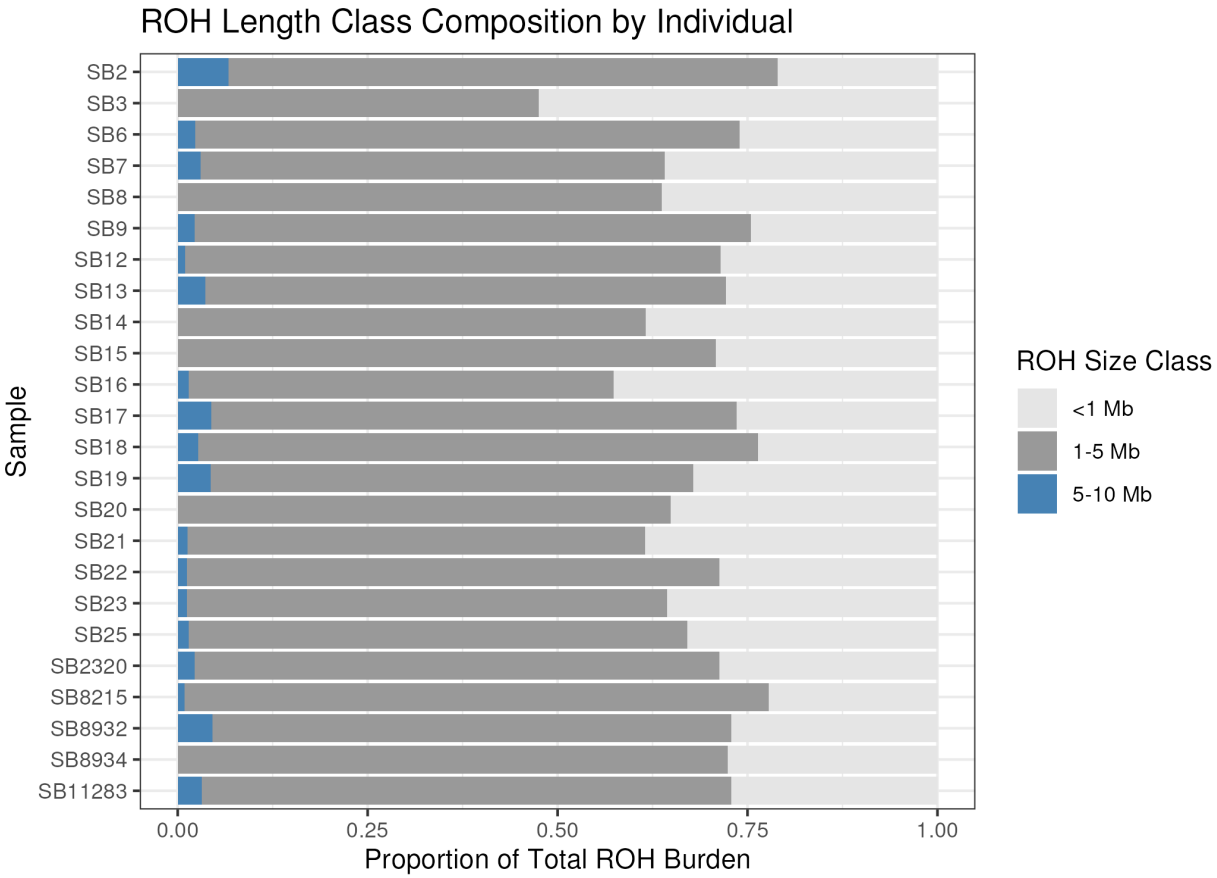

Figure 3-9. Proportion of ROH by size class in each individual, sorted by Studbook number.

Patterns of ROH across the genome are shown in Figure 3-10, ordered from lowest density at the top. Highest ROH densities appear in the modern descendants, and SB# 2.

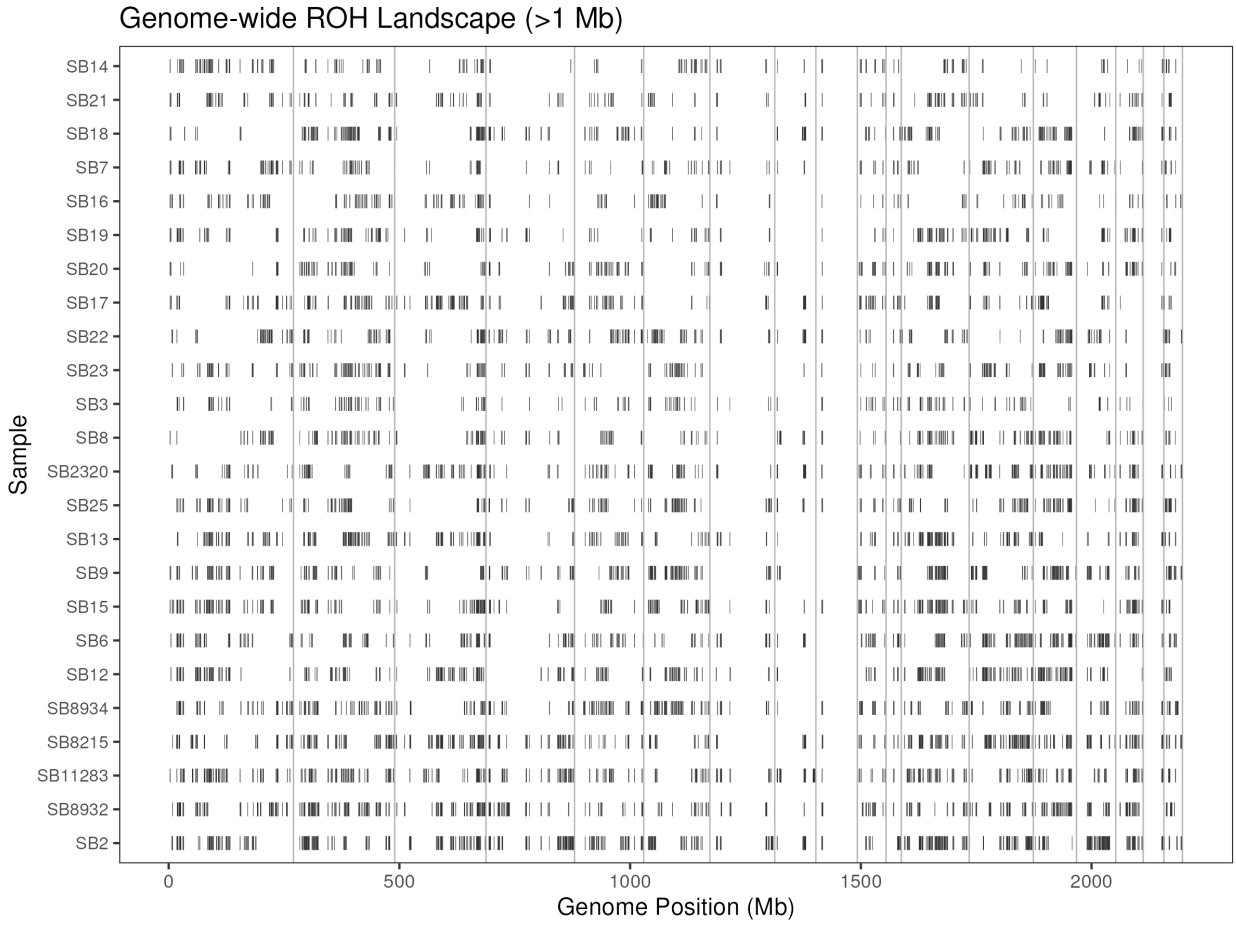

Figure 3-10. ROH across the genome, ordered by F_{ROH}.

3.4 PCA and Kinship

To visualize shared axes of variation, we conducted principal component analysis (PCA) on all 24 individuals as well as just the Meeteetse source population subset (n = 19). In the source population dataset, filtering for minor allele frequencies (MAF) less than 0.05 (which with this sample size basically aligns to just singleton variants) allowed us to see some population substructure within the high levels of background relatedness (Figure 3-11). Jenny (SB#17) and her litter (SB# 19-21) tend to group closely together, sometimes with their assumed sire,

Scarface (SB# 18), as do Mom (SB# 22) and her kits (SB# 23 and 25). Assumed siblings SB# 6 and SB# 7 also tend to cluster together. Dexter (SB# 16) does not cluster near his assumed parents, SB# 8 and SB# 9.

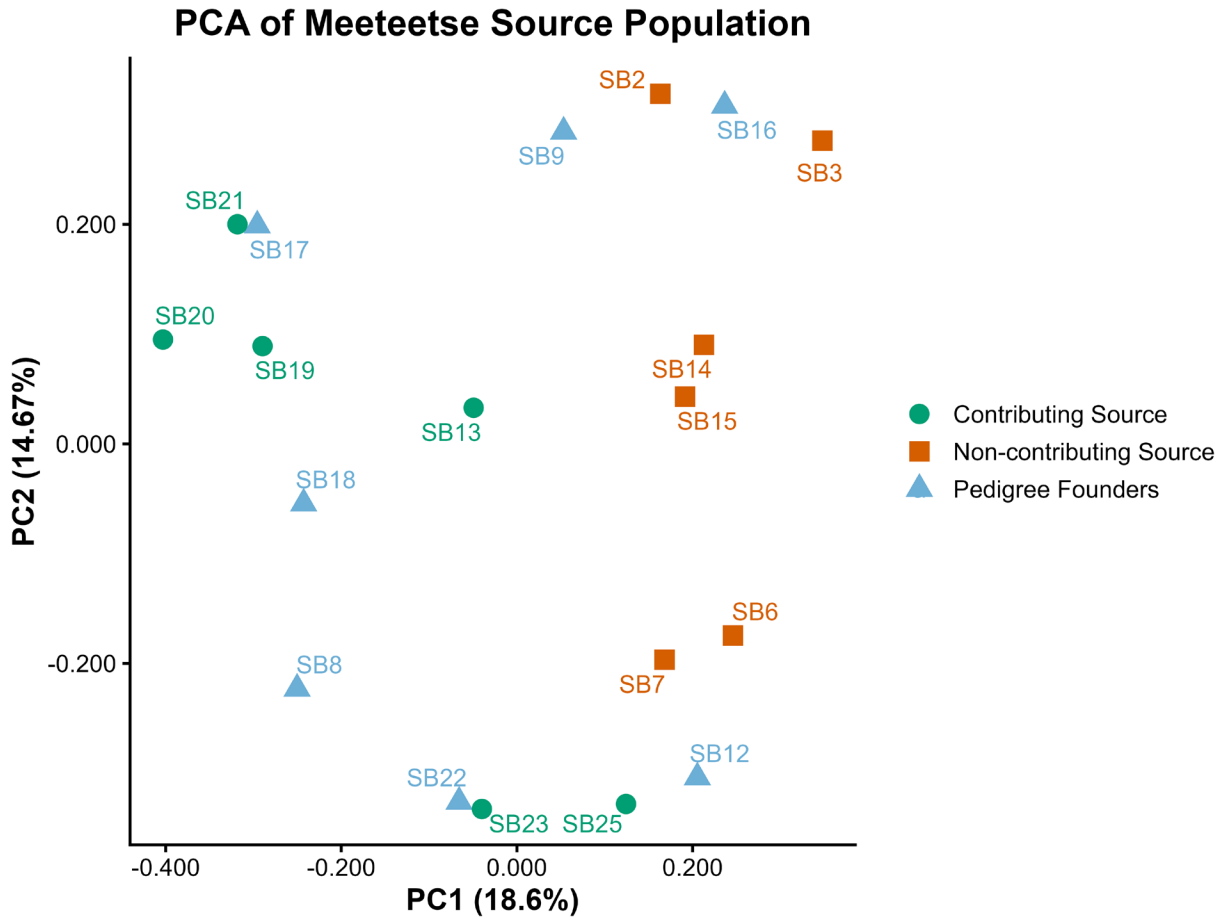

Figure 3-11. PCA for the 19 founders, maf = 0.05 (in this dataset, removes singletons).

Pedigree founders (the assumed seven genetic founders), contributing source ferrets (those offspring that bred and contributed genetically to the captive population), and non-contributing source ferrets (non-reproductive individuals) are color coded for comparison.

Visualizing PCA for all 24 samples, the descendants cluster tightly together on all principal component axes (Figure 3-12) along with major contributors to the extant population, especially SB# 13 (Dexter), SB# 17 (Jenny) and her kits, and SB#18 (Scarface). SB# 16 (Dean) tends to stay near the edges of both plots.

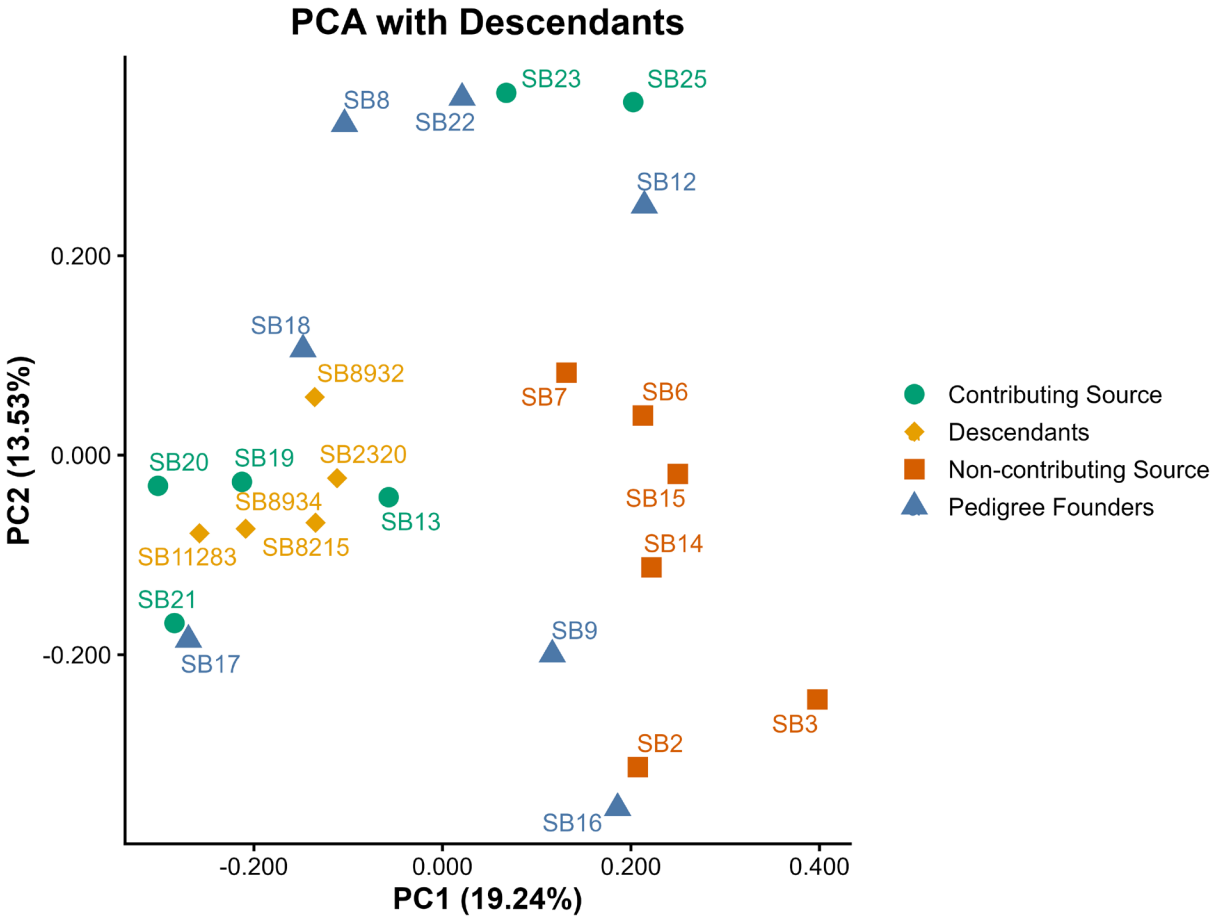

Figure 3-12. PCA for all 24 samples. MAF filter set to 0.05.

Analysis of high-quality SNP calls using PLINK2's KING function suggests the Meeteetse source population had a high level of background relatedness, especially as compared to the assumption that the genetic founders were all unrelated. Figure 3-13 compares expected pedigree pairwise kinship (lower triangle below the diagonal) with genomic-informed kinship (upper

triangle above the diagonal). Mean genomic kinship was 0.23 (SD = 0.04, range 0.14 to 0.33). The lowest reported kinship value in the table is 0.14—slightly exceeding the traditional expected kinship of half siblings (0.125). SB# 16 (Dean) stands out as the most unique individual with the lowest pairwise kinship coefficients (mean = 0.19).

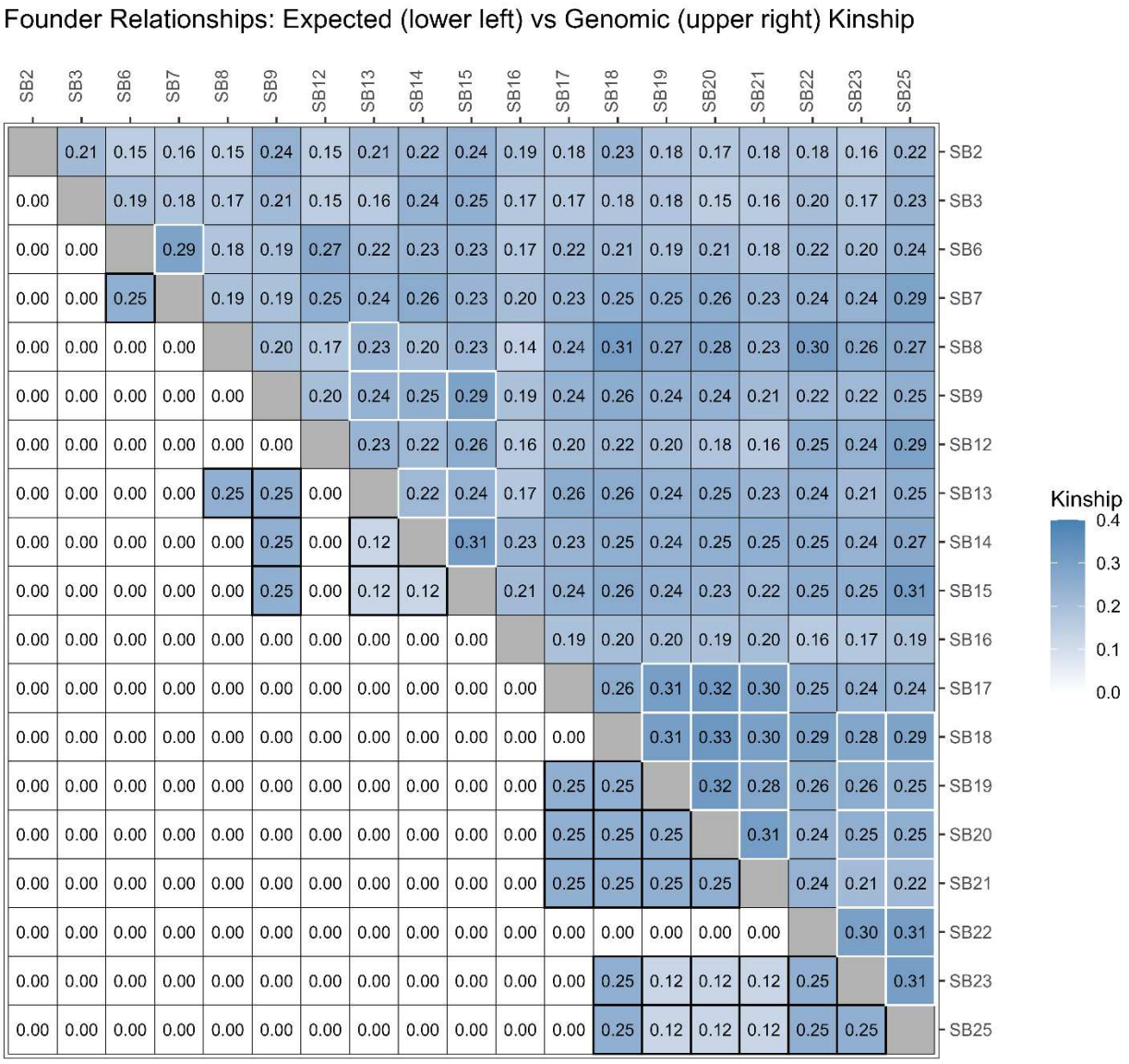

Figure 3-13. Kinship matrix for the 19 source population animals. Values below the diagonal are derived from the expected relationships from the initial assumed pedigree. Above the diagonal are the genomic-informed kinship estimates. Genomic values above the diagonal that mirror expected values below the diagonal are bordered in white.

Using a linear mixed-effects model controlling for repeated pairwise observations, we found that expected pedigree kinship was a positive predictor of genomic kinship among ferrets in the source population (β=0.225±0.032, t=6.95, Figure 3-14) and that including the expected kinship improved the model fit compared to the null (χ^2 = 41.4, df = 1, p<0.001). This indicates that the assumed pedigree is at least partially correct. Despite this relationship, the model intercept was high (β=0.220), suggesting a substantial level of baseline genomic relatedness among pairs within the source population, even though they were initially assumed to be unrelated.

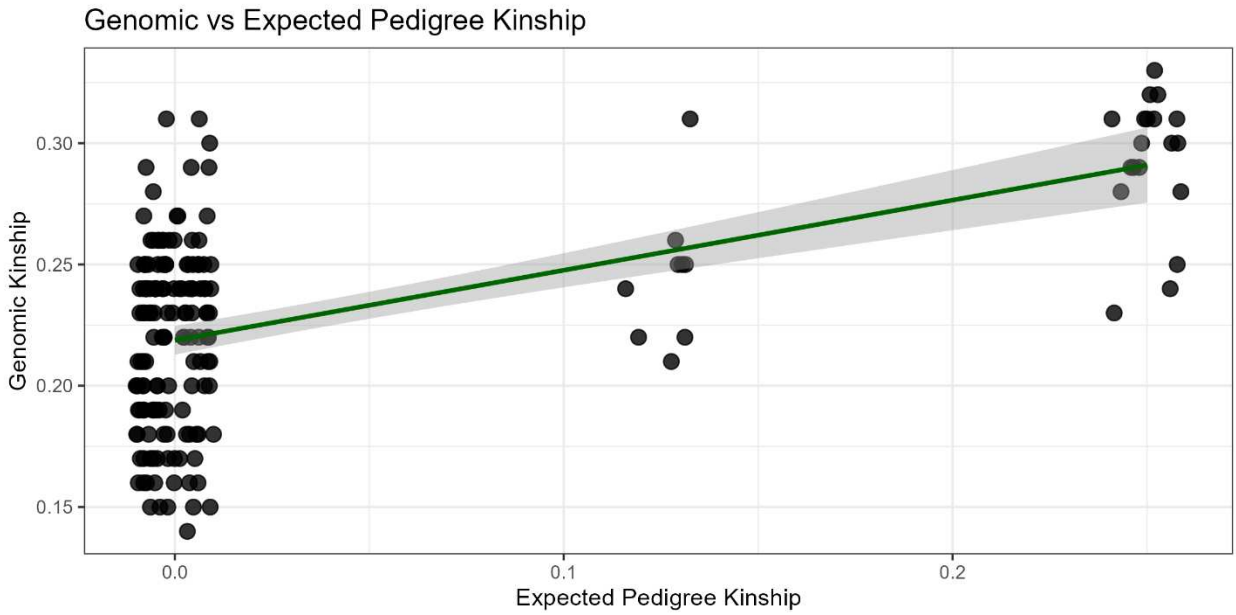

Figure 3-14. Genomic vs Expected pedigree kinship.

3.5 Sequoia

Pedigree inference was performed in Sequoia using a strictly filtered high-confidence SNP panel. Restricting analyses to SNP loci with low missingness (all SNP calls with high confidence in all individuals), that were unlinked (independent) and highly informative (minor allele frequency = 0.5) resulted in a final panel of 179 SNPs. Sequoia was able to test pedigree assumptions (Table

3.4) as well as reconstruct a partial *de novo* pedigree (Table 3.5). Positive log-likelihood ratios (LLR) indicate support for the proposed relationship, whereas negative values indicate poor support or contradictions.

Table 3.4. Test results from Sequoia with log-likelihood ratios based on relationships from the assumed pedigree.

Offspring	Dam	Sire	LLRdam	LLRsire	LLRpair	OHdam	OHsire	MEpair
SB6	WILD5	WILD4	0.84	0.84	0.13	NA	NA	NA
SB7	WILD5	WILD4	0.84	0.84	-3.34	NA	NA	NA
SB13	SB8	SB9	-49.23	-21.21	-65.72	3	3	24
SB14	NA	SB9	NA	-45.75	NA	NA	3	NA
SB15	NA	SB9	NA	-22.14	NA	NA	3	NA
SB19	SB17	SB18	2.04	3.25	6.75	0	0	0
SB20	SB17	SB18	1.36	0.04	2.91	0	0	1
SB21	SB17	SB18	1.57	-1.96	2.04	0	0	1
SB23	SB22	SB18	1.23	-18.39	-37.45	0	3	13
SB25	SB22	SB18	0.10	-99.87	-120.74	0	3	35

SB# 17 (Jenny) and SB# 18 (Scarface) had strong support as genetically compatible parents of SB#s 19-21 (LLRpair 2.04-6.75) despite a single Mendelian error (MEpair) for SB# 20 and 21. It is possible this is a sequencing or genotyping error, and there were no pairs of opposing homozygotes (OHdam/sire). SB# 22 (Mom) was moderately well supported as the dam for SB# 23 but marginally so as the dam for SB# 25. The presumed sire SB# 18 (Scarface) was not well supported for either offspring in this litter based on negative LLRs, multiple opposing homozygous loci, and Mendelian errors (MEpair 13-35, OHsire = 3). Sequoia returned negative LLRs for both parents of SB# 13 (Dexter), potentially elevating him to founder status. SB# 9 is also discounted as the sire for SB# 14 or 15.

Asked to infer relationships and reconstruct a pedigree without *a priori* parental identification, Sequoia returned the suggested relationships shown in Table 3.5. This inferred pedigree was then

evaluated using the same validation test applied to the expected pedigree (the CalcOHLLR function).

Table 3.5. Pedigree test results of the sequoia-inferred pedigree.

Offspring	Dam	Sire	LLRdam	LLRsire	LLRpair	OHdam	OHsire	MEpair
SB3	F0002	M0002	1.61	1.61	1.01	NA	NA	NA
SB6	F0002	M0002	1.61	1.61	-1.33	NA	NA	NA
SB12	F0001	M0001	0.00	0.00	3.55	NA	NA	NA
SB13	SB12	NA	-4.09	NA	NA	1	NA	NA
SB15	F0001	M0001	0.00	0.00	2.31	NA	NA	NA
SB19	SB17	SB18	1.51	3.25	4.68	0	0	0
SB20	SB17	SB18	1.36	0.04	1.84	0	0	1
SB21	SB17	SB18	1.57	-1.96	1.94	0	0	1
SB22	SB8	NA	2.70	NA	NA	0	NA	NA
SB23	SB22	NA	4.48	NA	NA	0	NA	NA
SB25	F0001	M0001	0.00	0.00	6.42	NA	NA	NA

Positive LLR values indicate greater support for the inferred relationship. OH values represent opposing homozygous loci between parent-offspring pairs and MEpair represents Mendelian incompatibilities across the inferred trio. Dummy parents (F000X/M000X) represent inferred parents not present in the dataset.

We see continued support for SB# 17 and 18's (Jenny and Scarface) family group. When the model was permitted to consider other potential sires (although none were definitively identified), support for SB# 22 (Mom) as the dam of SB#23 increased. Conversely, support shifted (LLRpair = 6.42) to a different parent pair for SB# 25 (Rene), potentially shared with SB# 12 (Annie) and SB# 15. Sequoia also supported SB# 8 as a potential dam of SB# 22 (LLRdam = 2.70) – a plausible relationship given that SB# 8 was recorded as an adult as early as 1984.

Differentiating between parental and full-sibling relationships is inherently challenging, as both share approximately the same proportion of identical-by-descent DNA (Thompson 1976). Consequently, given these algorithmic limitations, the reliance on estimated birth years for these

wild-caught individuals, and the high likelihood of interrelatedness among source ferrets in this area, the inferred pedigree presented in Table 3.5 should be interpreted as evidence of close familial associations rather than definitive parent-offspring ties.

3.6 Retained Variation

Whether alleles detected in the Meeteetse source population survived into descendant generations followed classical expectations of drift and fixation in small populations (Allendorf et al. 2022). We compared initial allele frequencies of polymorphic sites in the source population to their evolutionary fate in the descendant group, including retention of polymorphism, loss of the ALT allele compared to the REF allele, or fixation of the ALT allele. Rare variants were highly susceptible to loss through drift, while a smaller proportion of high-frequency alleles went to fixation (Figure 3-15). Sites fixed for the ALT allele in the source population (n = 8,081; AF = 1) remained fixed in descendant populations.

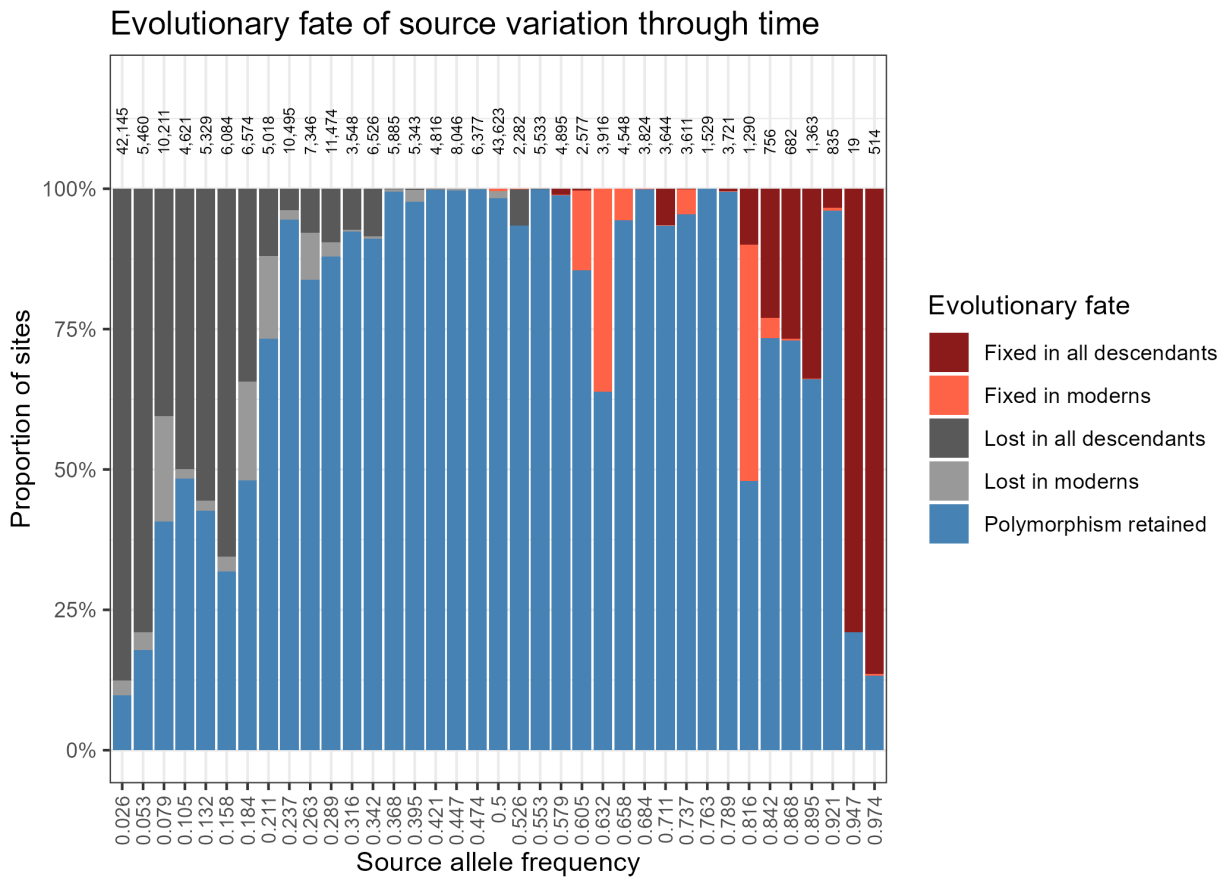

Figure 3-15. Evolutionary fate of founder alleles by starting allele frequency in the source population.

Considering SB# 2320 as an intermediate descendant between the source population and the modern population, patterns of allele retention suggest continued erosion of variation between 1998 and the present (Table 3.6). Although sample size for descendant individuals was limited, the observed patterns were consistent with expectations of progressive allelic loss caused by drift and non-breeding individuals in a closed population over time.

Table 3.6. Number and proportion of ALT alleles lost, fixed, or retained as polymorphism between all descendants and modern descendants only (SB# 2320 removed).

Population	ALT fixed	ALT lost	Polymorphism retained
All descendants (5)	1,749 (0.007)	60,532 (0.248)	182,179 (0.745)
Modern descendants (4)	4,708 (0.019)	67,869 (0.278)	171,883 (0.703)

3.7 Private Alleles

We assessed private alleles among individuals from the source population as an estimate of unique variation, with a focus on assumed and potential founders. We defined a 'private allele' as any locus where only a single individual was sequenced for the alternate (ALT) allele, and all other samples mapped to the reference (REF) allele. To reduce the likelihood that an allele might appear unique because it was masked by missingness in other samples, we required all SNPs in the 19 source ferrets from Meeteetse to be 100% callable across all individuals. Of 530,090 autosomal site-and genotype-filtered SNPs, 255,065 had complete genotype calls in all 19 source individuals. Of these, 42,438 (16.6%) were ALT alleles that differed from Capone's reference genotypes and were detected in only one source ferret. We then looked to see what proportion of these alleles were found in any of the five descendants (retention rate). The criterion of strict missingness was not enforced in the descendant samples to increase the likelihood of detecting a transmitted ALT allele.

As the private alleles analysis proved to be sensitive to whether closely related individuals were included in the dataset, we looked at unique variation among two subsets of the source population: The original seven presumed founders, and eight potential founders that were identified by our analyses of pedigrees and founders (Table 3.7).

Table 3.7. Private alleles and descendant retention detected in the original seven assumed founders, and the potential eight identified by analyses by Sequoia of the pedigree of the source population.

	Original 7 Founders		Potential 8 Founders	
Individual	Private alleles	Retention	Private alleles	Retention
SB8	2540	0.019	2533	0.013
SB9	2323	0.126	*NA*	*NA*
SB12	1650	0.043	2446	0.021
SB13	*NA*	*NA*	3158	0.472
SB16	20721	0.386	20856	0.343
SB17	4899	0.664	6305	0.727
SB18	2499	0.345	2133	0.24
SB22	1674	0.371	1563	0.343
SB25	*NA*	*NA*	832	0.066

SB# 16 (Dean) stands out with the highest private allele count—approximately 3x – 10x more than any other individual. SB# 8 and 9 have very little to no allelic retention in the descendants, but their assumed son SB# 13 (Dexter) does, supporting conclusions from Sequoia that they are not his parents and that Dexter is a true founder. SB# 25, identified by Sequoia as a potential founder, assuming her true parents are unsampled, shows the lowest unique allele count and a low retention rate. SB# 12 (Annie), a known founding breeder but who produced few offspring, also has low retention.

Although not directly comparable, the known breeding founders (if SB# 13 Dexter is substituted for SB#s 8 and 9) display allelic retention rates that are somewhat consistent with expectations of pedigree-based genetic representation from the studbook (Figure 3-16). The most noticeable outlier is SB# 18 (Scarface)—his allelic retention appears to be much lower than predicted based on the studbook. In addition to his variation being widely shared among other individuals of the source population, we surmise that Scarface's private allele counts were strongly limited by reference bias, as the sequenced reference animal Capone (SB#6536) was his direct offspring via artificial insemination. We would expect a large portion of Scarface's unique variation to map to the REF allele and thus depress his private allele count and retention rate.

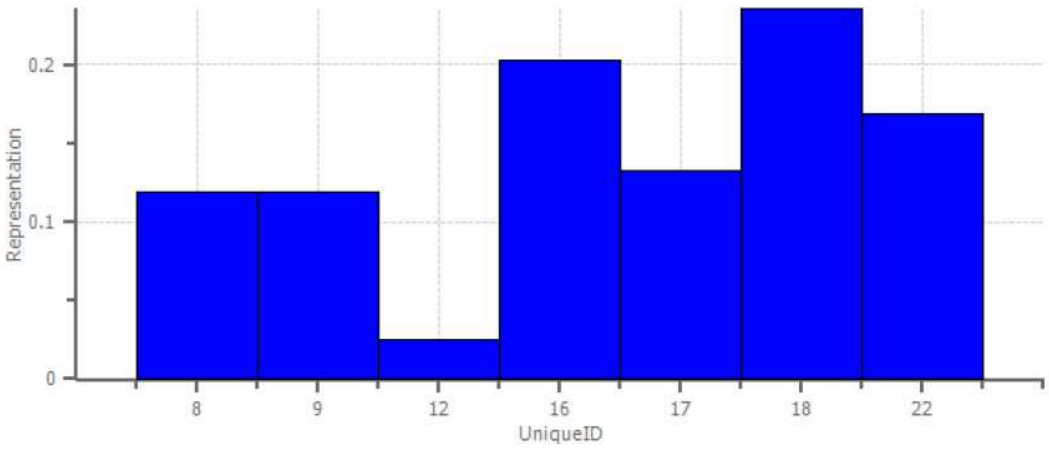

Figure 3. *Founder representation distribution of the Black-footed Ferret SSP population.*

Figure 3-16. Modeled pedigree-based genetic representation of the presumed founders from the 2022 AZA Black-footed Ferret SSP Breeding and Transfer Plan (Marinari and Lynch 2022).

CHAPTER 4: DISCUSSION

4.1 Genomic Diversity

Overall, our results show that the founding black-footed ferrets and their sampled descendants display low genome-wide heterozygosity, high levels of F_{ROH}, little differentiating variation apart from a single individual (SB# 16, Dean), and high levels of background relatedness. If we consider that every known black-footed ferret alive today is descended from this population, we can tentatively draw conclusions about the extant species. Taking into account that estimates of most genomic metrics can vary based on method and bioinformatic pipeline, black-footed ferret genome-wide autosomal heterozygosity (0.000027 – 0.000036) ranks among the lowest reported for any mammal. These values fall close to an order of magnitude below those reported for other threatened species, including African cheetahs (0.00019 – 0.00021; Dobrynin et al. 2015), Channel island foxes (0.0000142 – 0.000408; Robinson et al. 2016), and the recently reported Scottish population of the Eurasian red squirrel (0.00013 – 0.000325; Marr et al. 2025).

The proportion of the black-footed ferret genome contained in ROH follows a similar pattern, with a mean F_{ROH} across all samples of 0.2084. This is high, again compared to the red squirrel (mean = 0.0977 (Marr et al. 2025)) but not exceeding that of some Scandinavian wolves (mean = 0.27, highest F_{ROH} reported 0.54; Kardos et al. 2018), although we note that the latter results were based on analyses that used a more sophisticated measure of F_{ROH} that accounted for long ROH segments arising from inbreeding among more recent ancestors.

Neither of these results are surprising given the context of the ferrets' demographic history. The source population from Meeteetse likely suffered from genetic isolation and drift even before the rest of the species' range was extirpated. The bottleneck resulting from the extreme founder effect created when the Meeteetse population dwindled from ~120 individuals to a few genetic founders over just a few years in the early 1980s would have further reduced genetic diversity. However, as most ROH segments clustered in shorter to moderate size classes near 1Mb and the deficit of ROH segments >5Mb suggests that the majority of the ferrets' F_{ROH} arises from older patterns of population contraction and expansion rather than recent inbreeding. Coupled with the result that the difference in mean heterozygosity between the source population and modern descendants **(**Figure 3-1) was not significant suggests that the black-footed ferret recovery program has done an admirable job over the last 40 years in their mission to preserve as much existing genome-wide variation in this species as possible.

4.2 Pedigree and Kinship

One of the most striking results from this study is the estimated high level of background kinship in the source population relative to what is implied by the pedigree, especially among ferrets assumed to be unrelated (Figure 3-13). The intercept from our linear regression (Figure 3-14) suggests that for pairs of individuals with an expected kinship of 0, their predicted genomic kinship is 0.22—just under the expected kinship of full siblings (0.25). Overall genomic kinship ranged from 0.14 – 0.33 (mean = 0.23, SD = 0.04). Genomic kinships for expected sibling and parent-offspring pairs ranged from 0.28 – 0.33 (mean = 0.31, SD = 0.01), as would be expected or a little higher. However, genomic kinship for assumed unrelated pairs ranged between 0.14 and 0.31 (mean = 0.22, SD = 0.04), a considerable deviation from zero. The discrepancy between

expected and genomic kinship was significantly greater among pairs assumed to be unrelated than among first-degree relatives (Wilcoxon rank-sum test, $W = 0$, $p < 0.001$). Considering our other results and the species' population history, a non-zero baseline of relatedness in the source population is not surprising.

Our estimates of kinship among source population individuals allowed us to examine what possibilities for pairing existed when the captive population was initiated. In this scenario, we treat SB# 22 (Mom) and SB# 13 (Dexter) as founders but exclude SB# 8 because she died shortly after capture and did not contribute offspring. Figure 4-1 shows a breeding-style matrix with the pairwise kinships of all males and females known to have successfully bred and produced offspring in captivity. We excluded kits SB# 24, 26, and 27 as no archived tissues are known to exist from these individuals. These kinship values represent the relatedness of the pairs that would have been available at the start of the captive breeding program, but not necessarily the pairings that took place. Pairings with SB# 16 (Dean), the most genetically unique founder, would all still be at the level of first cousins or half-siblings. The others are all at the level of parent-offspring or full-sib matings. These findings demonstrate that the founders were already highly related at the onset of captive breeding, highlighting the limitations of assuming unrelated founders in conservation pedigrees. Such assumptions are common in conservation breeding programs initiated from small bottlenecked populations, despite often being biologically unrealistic (Galla et al. 2020).

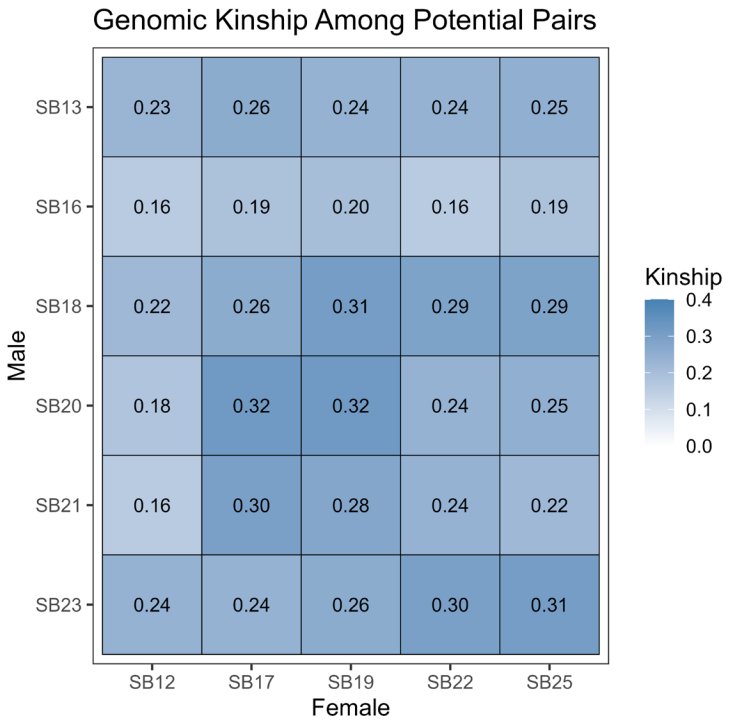

Figure 4-1. Genomic kinship from PLINK2's KING for pairs of source population individuals that were known to be reproductive after being brought into captivity. The matrix is missing SB#s 24, 26, and 27 as we could not locate samples from these individuals.

Our analysis of both the assumed pedigree and a pedigree derived only from genomic analysis helped elucidate the genetic founders for the black-footed ferret population. We confirmed founder status for SB# 12 (Annie), SB# 16 (Dean), SB# 17 (Jenny), and SB# 18 (Scarface). Dexter (SB# 13) becomes the new founder in place of SB# 8 and 9 as they are clearly not his parents, with a highly negative LLR for the trio (-65.72) and multiple opposing homozygotes for both parents. However, if we accept that SB# 8 is the dam of SB# 22 (Mom), then SB# 8 replaces SB# 22 as a founder. This relationship is plausible, as SB# 8 was the oldest confirmed ferret in the colony and was documented as an adult in 1984. On the other hand, it is also possible that SB# 8 and Mom were sisters, in which case Mom would remain the founder.

Sequoia also supported many of the relationship patterns identified using the KING estimator of kinship. Sequoia indicated a single Mendelian error between Scarface (SB# 18) and two of his assumed kits with Jenny (SB#s 20 and 21), but Sequoia also returned positive LLRs ranging from 2.04 to 6.75 for all three (SB# 19, 20, and 21) parent-offspring trios in this family group. These individuals also shared some of the highest kinship coefficients observed in the dataset (> 0.30), making it highly likely that Scarface (SB# 18) and Jenny (SB# 17) are indeed the parents of Becky (SB#19), Rocky (SB# 20), and Sundance (SB#21).

In contrast, Sequoia did not support Scarface as the sire of Mom's kits SB# 23 (Cutlip) or SB# 25 (Rene) (OHsire = 3 in all cases). Because male black-footed ferrets do not participate in kit rearing, it is plausible that a different but undetected male sired one or both of the SB# 23 and 25 kits. This male would represent a potential unidentified founder and source of unique variation. The result that SB# 23 (Cutlip) was Mom's offspring but SB# 25 (Rene) was not is also biologically plausible. Recent microsatellite-based research in free-ranging reintroduced black-footed ferrets in South Dakota demonstrated that litters captured from the same burrows may have mixed paternity, females may adopt or foster kits from other litters, and males may travel long distances to breed (Gibson 2025). This flexible reproductive system suggests that SB# 25 (Rene) may also have been a founder, but with undetected parents.

Sequoia also identified several previously unrecognized relationships. For example, SB# 12 (Annie), SB# 15, and SB# 25 (Rene) may share the same pair of undetected parents. However, these individuals were born in different years, and given what is known about ferret breeding, it is unlikely that the same breeding pair produced litters during three consecutive breeding

seasons. These high genomic similarities could also arise because of the high level of inbreeding in previous generations.

4.3 Private Alleles and Reference Bias

Analysis of private alleles showed that SB# 16 (Dean) was the most unique individual in the source population dataset by a large margin, with 3-10x the number of private alleles than any other individual. Most other ferrets have similar numbers of private alleles, as expected because they were all captured in close proximity on the original Meeteetse prairie dog colonies (Figure 1-2). The proportions of unique variation retained in descendants also aligned surprisingly well with founder representation projections from the modeled pedigree (Figure 3-16, Table 3.7). Studbook # 13 (Dexter) (standing in for 8 and 9), SB# 16 (Dean), and SB# 22 (Mom) are well represented, and SB# 17 (Jenny) appears to have been especially productive. Her direct offspring were themselves highly productive during the initial generations of captive breeding, producing a total of 46 surviving progeny (plus four more from Jenny) as Jenny's lineage escaped the bottleneck. Studbook #12's (Annie) contribution is expectedly low, as she produced only one surviving female offspring that successfully bred and contributed to the captive population.

The genetic legacy of Scarface (SB# 18; Table 3.7) measured through private alleles and retention, appears to be quite low and contradicts the higher estimates from the studbook pedigree (Figure 3-16). This could arise because Scarface was incorrectly assumed to be the sire of more ferrets in the captive breeding population (e.g., SB# 22 Mom's kits) when his initial contribution was much lower. Another reason is genome reference bias. Capone (SB#6536) was

the son of founder Scarface through artificial insemination and thus many of Scarface's actual private alleles would bioinformatically be scored as REF rather than ALT. The choice of reference genome, including its quality and level of genetic similarity to the population under study, can have noticeable impacts on downstream genomic analyses (Günther and Nettelblad 2019; Ahmad et al. 2025). Most of our bioinformatic analyses were made possible by having access to the recently published, high-quality chromosomal-level reference assembly for the black-footed ferret (Kliver et al. 2023). Read mapping success to the reference was excellent (>99%) because of the reference quality and the high genomic similarity of the reference individual and our sampled individuals. For Scarface in particular, many of his private alleles would have mapped to the REF allele. This bias may help explain why Scarface exhibited lower retained private allele proportions than expected despite pedigree projections that he contributed the largest proportion of ancestry to the extant population.

In addition to the reference bias, batch effects may have affected detection of private alleles. Some SNPs were seen in descendants but not the founders (between 318 and 804 private SNPs per descendant). All the descendants were sequenced at a higher coverage than the founders and had lower missingness. We also did not filter missingness strongly in the descendants, to detect as many alleles that were passed on as possible. Sites with high proportions of missingness would have been filtered out previously by requiring all the founders to have complete genotype calls. There was likely some detection asymmetry where alleles lost to missingness in the founders were 'rediscovered' in the higher quality descendant sequences. The less probable explanation is that private alleles in the descendants arose as *de novo* mutations. It is also possible that we did not sample additional private alleles from the source population because we

could only acquire and sequence samples from two of the five kits in SB# 22's (Mom) litter, and because the identity of Mom's mate is now under question and some private alleles were inherited from individuals who are not in the dataset.

4.4 Limitations and Recommendations

Downstream genomic analytics are sensitive to filtering choices (Hendricks et al. 2018) and this was apparent in many of our analyses. Using SNP sets prior to genotype quality and depth filtering with PLINK2's KING resulted in much lower pairwise kinship (-0.006 – 0.188; analysis not shown) that didn't align with the population history. Compared to the starting datasets, genotype depth, quality, and missingness filters improved Ts/Tv ratios (Table 3.1) and reduced Mendelian errors between likely related individuals (Table 3.4 and Table 3.5). This suggests the genotype filters helped to select SNPs that were appropriate for population analyses and removed spurious SNP calls.

Another limitation in this study was small sample size. Representation of the source population was good with 19 of 24 founding individuals providing high quality sequences. However, budget and time constraints only allowed the sampling of five descendant animals. A larger representation of individuals at different time points in the captive breeding effort would allow expanded analyses on the patterns of genetic diversity loss and retention over time and inform a more accurate picture of the current state of genomic diversity in this species. This could more accurately identify individuals that carry surviving rarer variation, such as the low-frequency alleles found in SB# 16 (Dean), than is possible from considering the pedigree alone. Sampling

known parents and their offspring would provide additional validation metrics for relationship inference, improving the results from this study.

The black-footed ferret recovery program uses the population management software package PMx (Lacy et al. 2012) in conjunction with breeding partners at AZA to make pairing recommendations and manage population demographics. We suggest incorporating the genomic kinships identified in this study as overlays in PMx to evaluate their effects on pairing recommendations. Although balancing founder representation this far into the pedigree is not practical as those lineages are now tied together after 40 years of captive breeding, it might better inform the distribution of unique variation throughout the pedigree.

We discovered that the founding black-footed ferrets came from an isolated population with high relatedness among individuals and little unique variation. Patterns of inbreeding were apparent with high proportions of the genome in runs of homozygosity, and genome-wide heterozygosity ranks among some of the lowest reported in any mammal. Some founder and pedigree assumptions were validated, while other assumed parent-offspring relationships and founders were not supported by genomic evidence, but clear evidence of additional founders was uncovered. Despite this, biologists over the past 40 years have succeeded in retaining an impressive amount of the starting variation available in the Meeteetse source population and building a successful recovery program. The results of this study will provide further insight into the genomic characteristics of the population and provide data to make genetically-informed breeding decisions in the future.

REFERENCES

Ahmad B et al. 2025. Mango pangenome reveals dramatic impacts of reference bias on population genomic analyses. Horticulture Research. 12(9):uhaf166. https://doi.org/10.1093/hr/uhaf166

Allendorf FW et al. 2022. Conservation and the Genomics of Populations. Oxford University Press. [accessed 2026 May 26]. https://doi.org/10.1093/oso/9780198856566.001.0001. https://doi.org/10.1093/oso/9780198856566.001.0001

Anderson E, Forrest S, Clark T, Richardson L. 1986. Paleobiology, biogeography, and systematics of the black-footed ferret, *Mustela nigripes* (Audubon and Bachman), 1851. Great Basin Naturalist Memoirs. 8(1) https://scholarsarchive.byu.edu/gbnm/vol8/iss1/3

Andrews S. 2010. FastQC: A Quality Control Tool for High Throughput Sequence Data [Online]; [accessed 2026 Apr 8]. https://www.bioinformatics.babraham.ac.uk/projects/fastqc/

Bates D, Mächler M, Bolker B, Walker S. 2015. Fitting Linear Mixed-Effects Models Using lme4. Journal of Statistical Software. 67:1–48. https://doi.org/10.18637/jss.v067.i01

Baughman J, Bortner R, Lynch C. 2026. AZA SAFE Program Population Analysis and Breeding and Transfer Plan for Black-footed Ferret (Mustela nigripes). AZA Population Management Center.

Belle EMS, Piganeau G, Gardner M, Eyre-Walker A. 2005. An investigation of the variation in the transition bias among various animal mitochondrial DNA. Gene. 355:58–66. https://doi.org/10.1016/j.gene.2005.05.019

Biggins DE, Godbey JL. 2003. Challenges to reestablishment of free-ranging populations of black-footed ferrets. Comptes Rendus Biologies. 326(S1):104–111. https://doi.org/10.1016/S1631-0691(03)00046-5

Campbell TM et al. 1987. Food Habits of Wyoming Black-footed Ferrets. The American Midland Naturalist. 117(1):208–210. https://doi.org/10.2307/2425722

Chang CC et al. 2015. Second-generation PLINK: rising to the challenge of larger and richer datasets. Gigascience. 4(1):s13742-015-0047–8. https://doi.org/10.1186/s13742-015-0047-8

Chen S. 2025. fastp 1.0: An ultra-fast all-round tool for FASTQ data quality control and preprocessing. [accessed 2026 Apr 7]. https://onlinelibrary.wiley.com/doi/10.1002/imt2.70078. https://doi.org/10.1002/imt2.70078

Danecek P et al. 2011. The variant call format and VCFtools. Bioinformatics. 27(15):2156–2158. https://doi.org/10.1093/bioinformatics/btr330

Danecek P et al. 2021. Twelve years of SAMtools and BCFtools. Gigascience. 10(2):giab008. https://doi.org/10.1093/gigascience/giab008

Dobrynin P et al. 2015. Genomic legacy of the African cheetah, Acinonyx jubatus. Genome Biol. 16(1):277. https://doi.org/10.1186/s13059-015-0837-4

Eads DA, Biggins DE, Livieri TM, Millspaugh JJ. 2014. Space use, Resource Selection and Territoriality of Black-Footed Ferrets: Implications for Reserve Design. Wildlife Biology. 20(1):27–36. https://doi.org/10.2981/wlb.13070

Ewels P, Magnusson M, Lundin S, Käller M. 2016. MultiQC: summarize analysis results for multiple tools and samples in a single report. Bioinformatics. 32(19):3047–3048. https://doi.org/10.1093/bioinformatics/btw354

Forrest SC et al. 1988. Population Attributes for the Black-Footed Ferret (Mustela nigripes) at Meeteetse, Wyoming, 1981-1985. Journal of Mammalogy. 69(2):261–273. https://doi.org/10.2307/1381377

Galla SJ et al. 2020. A comparison of pedigree, genetic and genomic estimates of relatedness for informing pairing decisions in two critically endangered birds: Implications for conservation breeding programmes worldwide. Evolutionary Applications. 13(5):991–1008. https://doi.org/10.1111/eva.12916

Gibson MR. 2025. Genetic evaluation of the mating system in an endangered carnivore. Central Michigan University. [accessed 2026 June 3]. https://scholarly.cmich.edu/?a=d&d=CMUGR2025-059.1.6&e=-------en-10--1--txt-txIN%7CtxAU%7CtxTI--------

Godbey JL, Biggins DE, Garelle D. 2006. Exposure of Captive Black-footed Ferrets to Plague and Implications for Species Recovery. In Recovery of the Black-footed Ferret: Progress and Continuing Challenges. Edited by J.E. Roelle, B.J. Miller, J.L. Godbey, and D.E. Biggins. U.S. Geological Survey p 233–237. Report No.: 2005–5293. https://doi.org/10.3133/sir20055293

Günther T, Nettelblad C. 2019. The presence and impact of reference bias on population genomic studies of prehistoric human populations. PLOS Genetics. 15(7):e1008302. https://doi.org/10.1371/journal.pgen.1008302

Hendricks S et al. 2018. Recent advances in conservation and population genomics data analysis. Evolutionary Applications. 11(8):1197–1211. https://doi.org/10.1111/eva.12659

Hillman CN. 1968. LIFE HISTORY AND ECOLOGY OF THE BLACK-FOOTED FERRET IN THE WILD. South Dakota State University.

Huisman J. 2017. Pedigree reconstruction from SNP data: parentage assignment, sibship clustering and beyond. Molecular Ecology Resources. 17(5):1009–1024. https://doi.org/10.1111/1755-0998.12665

Jamieson IG. 2011. Founder Effects, Inbreeding, and Loss of Genetic Diversity in Four Avian Reintroduction Programs. Conservation Biology. 25(1):115–123. https://doi.org/10.1111/j.1523-1739.2010.01574.x

Kardos M et al. 2018. Genomic consequences of intensive inbreeding in an isolated wolf population. Nat Ecol Evol. 2(1):124–131. https://doi.org/10.1038/s41559-017-0375-4

Kardos M et al. 2021. The crucial role of genome-wide genetic variation in conservation. Proceedings of the National Academy of Sciences. 118(48):e2104642118. https://doi.org/10.1073/pnas.2104642118

Kardos M, Luikart G, Allendorf FW. 2015. Measuring individual inbreeding in the age of genomics: marker-based measures are better than pedigrees. Heredity. 115(1):63–72. https://doi.org/10.1038/hdy.2015.17

Kliver S et al. 2023. Chromosome-length genome assembly and karyotype of the endangered black-footed ferret (Mustela nigripes). Journal of Heredity. 114(5):539–548. https://doi.org/10.1093/jhered/esad035

Knaus BJ, Grünwald NJ. 2017. vcfr: a package to manipulate and visualize variant call format data in R. Molecular Ecology Resources. 17(1):44–53. https://doi.org/10.1111/1755-0998.12549

Korneliussen TS, Albrechtsen A, Nielsen R. 2014. ANGSD: Analysis of Next Generation Sequencing Data. BMC Bioinformatics. 15(1):356. https://doi.org/10.1186/s12859-014-0356-4

Lacy RC, Ballou JD, Pollak JP. 2012. PMx: software package for demographic and genetic analysis and management of pedigreed populations. Methods in Ecology and Evolution. 3(2):433–437. https://doi.org/10.1111/j.2041-210X.2011.00148.x

Manichaikul A et al. 2010. Robust relationship inference in genome-wide association studies. Bioinformatics. 26(22):2867–2873. https://doi.org/10.1093/bioinformatics/btq559

Marinari PaulE, Lynch C. 2021. AZA Black-footed Ferret SSP Breeding and Transfer Plan. AZA Population Management Center.

Marinari PaulE, Lynch C. 2022. AZA Black-footed Ferret SSP Breeding and Transfer Plan. AZA Population Management Center.

Marr MM et al. 2025. Genomic Insights Into Red Squirrels in Scotland Reveal Loss of Heterozygosity Associated With Extreme Founder Effects. Evolutionary Applications. 18(1):e70072. https://doi.org/10.1111/eva.70072

Matchett MR et al. 2010. Enzootic Plague Reduces Black-Footed Ferret (Mustela nigripes) Survival in Montana. Vector-Borne Zoonotic Dis. 10(1):27–35. https://doi.org/10.1089/vbz.2009.0053

Narasimhan V et al. 2016. BCFtools/RoH: a hidden Markov model approach for detecting autozygosity from next-generation sequencing data. Bioinformatics. 32(11):1749–1751. https://doi.org/10.1093/bioinformatics/btw044

Poplin R et al. 2018. Scaling accurate genetic variant discovery to tens of thousands of samples. 201178 [accessed 2026 Apr 15]. https://www.biorxiv.org/content/10.1101/201178v3. https://doi.org/10.1101/201178

Prunier JG, Veyssière C, Loot G, Blanchet S. 2023. Comparing the Utility of Microsatellites and Single Nucleotide Polymorphisms in Conservation Genetics: Insights from a Study on Two Freshwater Fish Species in France. Diversity. 15(5):681. https://doi.org/10.3390/d15050681

R Core Team. 2024. R: A Language and Environment for Statistical Computing. https://www.R-project.org/

Robinson JA et al. 2016. Genomic Flatlining in the Endangered Island Fox. Current Biology. 26(9):1183–1189. https://doi.org/10.1016/j.cub.2016.02.062

Rocke TE et al. 2008. Vaccination with F1-V fusion protein protects black-footed ferrets (Mustela nigripes) against plague upon oral challenge with Yersinia pestis. - Colorado State University. Journal of Wildlife Diseases. 44(1):1–7

Santymire RM et al. 2019. Inbreeding causes decreased seminal quality affecting pregnancy and litter size in the endangered black-footed ferret. Animal Conservation. 22(4):331–340. https://doi.org/10.1111/acv.12466

Santymire RM, Livieri TM, Branvold-Faber H, Marinari PE. 2014. The Black-Footed Ferret: On the Brink of Recovery? In: Holt WV, Brown JL, Comizzoli P, editors. Reproductive Sciences in Animal Conservation: Progress and Prospects. Springer; p 119–134 [accessed 2026 May 29]. https://doi.org/10.1007/978-1-4939-0820-2_7. https://doi.org/10.1007/978-1-4939-0820-2_7

Sheets RG, Linder RL, Dahlgren RB. 1972. Food Habits of Two Litters of Black-Footed Ferrets in South Dakota. The American Midland Naturalist. 87(1):249–251. https://doi.org/10.2307/2423900

Thompson EA. 1976. A Paradox of Genealogical Inference. Advances in Applied Probability. 8(4):648–650. https://doi.org/10.2307/1425927

Thompson EA. 2013. Identity by Descent: Variation in Meiosis, Across Genomes, and in Populations. Genetics. 194(2):301–326. https://doi.org/10.1534/genetics.112.148825

University of Colorado Boulder Research Computing. 2023. Alpine. University of Colorado Boulder; [accessed 2026 Apr 8]. https://www.colorado.edu/rc/alpine. https://doi.org/https://doi.org/10.25811/k3w6-pk81

U.S. Fish and Wildlife Service. 2013. Recovery plan for the black-footed ferret (Mustela nigripes). U.S. Fish and Wildlife Service p 157.

Van der Auwera GA, O'Connor BD. 2020. Genomics in the Cloud: Using Docker, GATK, and WDL in Terra. 1st ed. [accessed 2026 Apr 26]. https://www.oreilly.com/library/view/genomics-in-the/9781491975183/

Vasimuddin Md, Misra S, Li H, Aluru S. 2019. Efficient Architecture-Aware Acceleration of BWA-MEM for Multicore Systems. In: 2019 IEEE International Parallel and Distributed Processing Symposium (IPDPS). p 314–324 [accessed 2026 Apr 8]. https://ieeexplore.ieee.org/document/8820962. https://doi.org/10.1109/IPDPS.2019.00041

Wickham H. 2016. ggplot2: Elegant Graphics for Data Analysis. https://ggplot2.tidyverse.org

Wickham H et al. 2019. Welcome to the Tidyverse. Journal of Open Source Software. 4(43):1686. https://doi.org/10.21105/joss.01686

Williams ES et al. 1994. Plague in a Black-footed Ferret (Mustela nigripes). The Journal of Wildlife Diseases. 30(4):581–585. https://doi.org/10.7589/0090-3558-30.4.581

Williams ES, Thome ET, Appel MJG, Belitsky DW. 1988. CANINE DISTEMPER IN BLACK-FOOTED FERRETS (MUSTELA NIGRIPES) FROM WYOMING. The Journal of Wildlife Diseases. 24(3):385–398. https://doi.org/10.7589/0090-3558-24.3.385

Wisely SM, Statham MJ, Fleischer RC. 2008. Pleistocene Refugia and Holocene Expansion of a Grassland-Dependent Species, the Black-Footed Ferret (Mustela nigripes). J Mammal. 89(1):87–96. https://doi.org/10.1644/07-MAMM-A-077.1

Zimmerman SJ et al. 2025. Assessing shifting technology in genetic monitoring of the North American plains bison Federal conservation herds. Conserv Genet. 26(4):657–675. https://doi.org/10.1007/s10592-025-01694-2

APPENDICES

Output from Plink2 King. Filtering options in effect: GATK4: FORMAT/DP <5, FORMAT GQ < 20, Plink2: mac 1, geno 0.1, indep-pairwise 50 10 0.1

ID1	ID2	NSNP	HETHET	IBS0	KINSHIP
SB00016_MSB127012	SB00008_MVZ195115	17671	0.134458	0.027955	0.135896
SB00002_MVZ195117	SB00006_MSB127009	18766	0.140573	0.03128	0.148786
SB00012_MSB122103	SB00003_MVZ195118	17660	0.13641	0.027123	0.151333
SB00020_MSB122104	SB00003_MVZ195118	18065	0.14708	0.030944	0.151682
SB00002_MVZ195117	SB00012_MSB122103	18406	0.131751	0.027002	0.154317
SB00002_MVZ195117	SB00008_MVZ195115	18404	0.137796	0.024234	0.154554
SB00021_MSB122101	SB00012_MSB122103	17950	0.145181	0.025627	0.155187
SB00021_MSB122101	SB00003_MVZ195118	17814	0.141406	0.024644	0.159816
SB00002_MVZ195117	SB00007_MVZ195114	18624	0.131175	0.016269	0.160482
SB00016_MSB127012	SB00012_MSB122103	17673	0.126464	0.014938	0.162954
SB00002_MVZ195117	SB00023_MSB122102	18446	0.136019	0.020167	0.163659
SB00013_MSB127010	SB00003_MVZ195118	17969	0.135901	0.024542	0.163813
SB00022_MSB122110	SB00016_MSB127012	17771	0.136965	0.021608	0.164148
SB00017_MSB122108	SB00003_MVZ195118	17642	0.131221	0.022333	0.167056
SB00002_MVZ195117	SB00020_MSB122104	18811	0.141513	0.019829	0.167782
SB00008_MVZ195115	SB00003_MVZ195118	17658	0.146053	0.028203	0.170848
SB00023_MSB122102	SB00016_MSB127012	17713	0.127872	0.016033	0.171266
SB00016_MSB127012	SB00013_MSB127010	17982	0.135914	0.017907	0.172422
SB00023_MSB122102	SB00003_MVZ195118	17700	0.14887	0.028249	0.172835
SB00016_MSB127012	SB00003_MVZ195118	17537	0.127388	0.014769	0.173741
SB00016_MSB127012	SB00006_MSB127009	18033	0.13503	0.016803	0.174007
SB00012_MSB122103	SB00008_MVZ195115	17794	0.135102	0.021187	0.174041
SB00008_MVZ195115	SB00006_MSB127009	18154	0.140465	0.023962	0.175161
SB00020_MSB122104	SB00012_MSB122103	18201	0.143399	0.021482	0.175451
SB00021_MSB122101	SB00006_MSB127009	18310	0.145931	0.021682	0.177632
SB00019_MSB122105	SB00003_MVZ195118	17810	0.149579	0.025435	0.177797
SB00002_MVZ195117	SB00022_MSB122110	18504	0.139754	0.020698	0.180366
SB00002_MVZ195117	SB00021_MSB122101	18560	0.147091	0.018966	0.180548
SB00018_MSB122109	SB00003_MVZ195118	17910	0.151424	0.027973	0.181592
SB00007_MVZ195114	SB00003_MVZ195118	17878	0.146549	0.022877	0.182153
SB00002_MVZ195117	SB00019_MSB122105	18556	0.141086	0.01703	0.183058
SB00002_MVZ195117	SB00017_MSB122108	18388	0.138242	0.019089	0.183392
SB00019_MSB122105	SB00006_MSB127009	18306	0.150442	0.02338	0.186268
SB00016_MSB127012	SB00009_MVZ195113	17980	0.127753	0.010178	0.186478
SB00002_MVZ195117	SB00016_MSB127012	18283	0.132254	0.010173	0.187129
SB00025_MSB127011	SB00016_MSB127012	18303	0.144239	0.018904	0.189657
SB00020_MSB122104	SB00016_MSB127012	18078	0.137349	0.016097	0.190386

SB00006_MSB127009	SB00003_MVZ195118	18020	0.137292	0.018258	0.191725
SB00009_MVZ195113	SB00006_MSB127009	18463	0.135623	0.021611	0.193063
SB00017_MSB122108	SB00016_MSB127012	17655	0.138601	0.015067	0.193994
SB00009_MVZ195113	SB00007_MVZ195114	18321	0.146389	0.018776	0.194704
SB00008_MVZ195115	SB00007_MVZ195114	18012	0.154397	0.023984	0.194978
SB00018_MSB122109	SB00016_MSB127012	17923	0.142331	0.016348	0.197366
SB00022_MSB122110	SB00003_MVZ195118	17758	0.142584	0.020047	0.197563
SB00019_MSB122105	SB00016_MSB127012	17823	0.139651	0.014812	0.198941
SB00014_MSB122107	SB00008_MVZ195115	17805	0.152878	0.019938	0.2
SB00009_MVZ195113	SB00008_MVZ195115	18101	0.147506	0.02138	0.200724
SB00019_MSB122105	SB00012_MSB122103	17946	0.144378	0.016383	0.201091
SB00017_MSB122108	SB00012_MSB122103	17778	0.142479	0.0189	0.201628
SB00023_MSB122102	SB00006_MSB127009	18196	0.142944	0.017092	0.202899
SB00012_MSB122103	SB00009_MVZ195113	18103	0.139203	0.021157	0.202918
SB00016_MSB127012	SB00007_MVZ195114	17891	0.143368	0.015539	0.20305
SB00021_MSB122101	SB00016_MSB127012	17827	0.146014	0.016604	0.203789
SB00023_MSB122102	SB00013_MSB127010	18145	0.143952	0.016919	0.206851
SB00021_MSB122101	SB00009_MVZ195113	18257	0.149093	0.015611	0.208085
SB00002_MVZ195117	SB00013_MSB127010	18715	0.14085	0.018434	0.209635
SB00020_MSB122104	SB00006_MSB127009	18561	0.15942	0.02112	0.21159
SB00009_MVZ195113	SB00003_MVZ195118	17967	0.141203	0.015362	0.211623
SB00016_MSB127012	SB00015_MVZ195116	18177	0.140672	0.010618	0.212472
SB00023_MSB122102	SB00021_MSB122101	17990	0.146581	0.013785	0.213633
SB00002_MVZ195117	SB00003_MVZ195118	18270	0.138807	0.01248	0.214124
SB00018_MSB122109	SB00006_MSB127009	18406	0.153809	0.020265	0.214423
SB00022_MSB122110	SB00009_MVZ195113	18201	0.153893	0.021702	0.215127
SB00013_MSB127010	SB00006_MSB127009	18465	0.142215	0.018576	0.218395
SB00018_MSB122109	SB00012_MSB122103	18046	0.144076	0.014131	0.219313
SB00002_MVZ195117	SB00025_MSB127011	19036	0.146512	0.014656	0.220023
SB00025_MSB127011	SB00021_MSB122101	18580	0.164316	0.020937	0.220981
SB00014_MSB122107	SB00012_MSB122103	17807	0.144325	0.009266	0.221473
SB00021_MSB122101	SB00015_MVZ195116	18454	0.161591	0.018424	0.222826
SB00023_MSB122102	SB00009_MVZ195113	18143	0.151078	0.01637	0.223085
SB00017_MSB122108	SB00006_MSB127009	18138	0.14952	0.017698	0.2232
SB00022_MSB122110	SB00006_MSB127009	18254	0.147475	0.016654	0.223307
SB00002_MVZ195117	SB00014_MSB122107	18417	0.148504	0.010534	0.2236
SB00014_MSB122107	SB00013_MSB127010	18116	0.148819	0.011316	0.224234
SB00025_MSB127011	SB00003_MVZ195118	18290	0.159486	0.020776	0.225196
SB00021_MSB122101	SB00013_MSB127010	18259	0.154663	0.013966	0.226886
SB00017_MSB122108	SB00007_MVZ195114	17996	0.150756	0.013725	0.227024
SB00013_MSB127010	SB00012_MSB122103	18105	0.135101	0.012814	0.22708
SB00015_MVZ195116	SB00008_MVZ195115	18298	0.156957	0.019237	0.229341
SB00017_MSB122108	SB00014_MSB122107	17789	0.153915	0.012817	0.230378
SB00020_MSB122104	SB00015_MVZ195116	18705	0.160171	0.016947	0.230527
SB00021_MSB122101	SB00007_MVZ195114	18168	0.146191	0.009632	0.231047

SB00014_MSB122107	SB00006_MSB127009	18167	0.150658	0.010348	0.231769
SB00016_MSB127012	SB00014_MSB122107	17684	0.149966	0.010292	0.232427
SB00015_MVZ195116	SB00006_MSB127009	18660	0.141693	0.014791	0.232728
SB00002_MVZ195117	SB00018_MSB122109	18656	0.148907	0.012811	0.232813
SB00015_MVZ195116	SB00007_MVZ195114	18518	0.146452	0.009558	0.233603
SB00013_MSB127010	SB00008_MVZ195115	18103	0.141524	0.010717	0.233956
SB00021_MSB122101	SB00008_MVZ195115	17948	0.156953	0.013372	0.234182
SB00025_MSB127011	SB00017_MSB122108	18408	0.148577	0.013418	0.235128
SB00002_MVZ195117	SB00009_MVZ195113	18713	0.131032	0.008817	0.236067
SB00022_MSB122110	SB00021_MSB122101	18048	0.147329	0.007868	0.236675
SB00023_MSB122102	SB00007_MVZ195114	18054	0.16495	0.017614	0.236676
SB00017_MSB122108	SB00008_MVZ195115	17776	0.144239	0.01142	0.237249
SB00013_MSB127010	SB00007_MVZ195114	18323	0.149157	0.010206	0.237271
SB00002_MVZ195117	SB00015_MVZ195116	18910	0.140666	0.012956	0.237853
SB00013_MSB127010	SB00009_MVZ195113	18412	0.135401	0.010265	0.238223
SB00017_MSB122108	SB00009_MVZ195113	18085	0.138513	0.00846	0.238248
SB00023_MSB122102	SB00017_MSB122108	17818	0.148333	0.011674	0.238554
SB00014_MSB122107	SB00003_MVZ195118	17671	0.151152	0.008262	0.238716
SB00023_MSB122102	SB00014_MSB122107	17847	0.154368	0.010422	0.238985
SB00017_MSB122108	SB00015_MVZ195116	18282	0.142216	0.010119	0.239398
SB00022_MSB122110	SB00013_MSB127010	18203	0.138274	0.008295	0.239674
SB00019_MSB122105	SB00009_MVZ195113	18253	0.148743	0.009587	0.239849
SB00022_MSB122110	SB00007_MVZ195114	18112	0.160722	0.014631	0.241008
SB00023_MSB122102	SB00012_MSB122103	17836	0.148183	0.010092	0.242021
SB00015_MVZ195116	SB00013_MSB127010	18609	0.14047	0.01193	0.242128
SB00019_MSB122105	SB00014_MSB122107	17957	0.163223	0.014034	0.242627
SB00022_MSB122110	SB00020_MSB122104	18299	0.156511	0.011749	0.243142
SB00025_MSB127011	SB00006_MSB127009	18786	0.148302	0.010859	0.243423
SB00019_MSB122105	SB00013_MSB127010	18255	0.152725	0.010682	0.243603
SB00020_MSB122104	SB00009_MVZ195113	18508	0.162848	0.014967	0.244087
SB00019_MSB122105	SB00015_MVZ195116	18450	0.157019	0.012629	0.244182
SB00020_MSB122104	SB00014_MSB122107	18212	0.158302	0.011037	0.245253
SB00015_MVZ195116	SB00003_MVZ195118	18164	0.142314	0.007487	0.245512
SB00022_MSB122110	SB00012_MSB122103	17894	0.129205	0.002347	0.245779
SB00025_MSB127011	SB00013_MSB127010	18735	0.151321	0.011743	0.245855
SB00012_MSB122103	SB00007_MVZ195114	18014	0.14028	0.003109	0.246145
SB00025_MSB127011	SB00009_MVZ195113	18733	0.162441	0.017082	0.246936
SB00025_MSB127011	SB00020_MSB122104	18831	0.172322	0.019064	0.247139
SB00023_MSB122102	SB00015_MVZ195116	18340	0.14482	0.00747	0.247346
SB00023_MSB122102	SB00020_MSB122104	18241	0.160627	0.012993	0.24786
SB00022_MSB122110	SB00014_MSB122107	17905	0.16716	0.014242	0.248085
SB00021_MSB122101	SB00014_MSB122107	17961	0.159457	0.010746	0.248189
SB00022_MSB122110	SB00017_MSB122108	17876	0.143433	0.008559	0.248609
SB00014_MSB122107	SB00009_MVZ195113	18114	0.152148	0.006349	0.25069
SB00025_MSB127011	SB00019_MSB122105	18576	0.164836	0.014858	0.250724

SB00019_MSB122105	SB00007_MVZ195114	18164	0.164446	0.013598	0.251885
SB00018_MSB122109	SB00007_MVZ195114	18264	0.162505	0.012976	0.25272
SB00020_MSB122104	SB00013_MSB127010	18510	0.15705	0.009887	0.253071
SB00018_MSB122109	SB00014_MSB122107	18057	0.159883	0.009525	0.25401
SB00022_MSB122110	SB00015_MVZ195116	18398	0.15643	0.013588	0.254089
SB00023_MSB122102	SB00008_MVZ195115	17834	0.151564	0.008411	0.25561
SB00018_MSB122109	SB00009_MVZ195113	18353	0.156269	0.011115	0.256649
SB00018_MSB122109	SB00015_MVZ195116	18550	0.153261	0.009811	0.256832
SB00015_MVZ195116	SB00012_MSB122103	18300	0.14623	0.011093	0.257516
SB00020_MSB122104	SB00007_MVZ195114	18419	0.162169	0.01075	0.259309
SB00018_MSB122109	SB00013_MSB127010	18355	0.157832	0.011223	0.260178
SB00017_MSB122108	SB00013_MSB127010	18087	0.155526	0.011113	0.262315
SB00023_MSB122102	SB00019_MSB122105	17986	0.161292	0.009674	0.26275
SB00022_MSB122110	SB00019_MSB122105	18044	0.153181	0.005597	0.263336
SB00014_MSB122107	SB00007_MVZ195114	18025	0.162718	0.008266	0.263468
SB00018_MSB122109	SB00017_MSB122108	18028	0.158087	0.010373	0.264222
SB00012_MSB122103	SB00006_MSB127009	18156	0.1372	0.005232	0.266209
SB00019_MSB122105	SB00008_MVZ195115	17944	0.155985	0.005852	0.268815
SB00025_MSB127011	SB00008_MVZ195115	18424	0.16663	0.012918	0.269804
SB00025_MSB127011	SB00014_MSB122107	18437	0.16532	0.006997	0.273639
SB00021_MSB122101	SB00019_MSB122105	18100	0.166298	0.005801	0.279953
SB00020_MSB122104	SB00008_MVZ195115	18199	0.162427	0.00478	0.281423
SB00023_MSB122102	SB00018_MSB122109	18086	0.160345	0.005916	0.283528
SB00025_MSB127011	SB00007_MVZ195114	18644	0.168472	0.007026	0.285825
SB00015_MVZ195116	SB00009_MVZ195113	18607	0.154082	0.007793	0.287393
SB00022_MSB122110	SB00018_MSB122109	18144	0.165068	0.006889	0.288769
SB00025_MSB127011	SB00018_MSB122109	18676	0.175037	0.011994	0.289162
SB00025_MSB127011	SB00012_MSB122103	18426	0.157983	0.003636	0.293315
SB00007_MVZ195114	SB00006_MSB127009	18374	0.168445	0.005769	0.294071
SB00021_MSB122101	SB00017_MSB122108	17932	0.164455	0.000725	0.297492
SB00021_MSB122101	SB00018_MSB122109	18200	0.16456	0.00044	0.299717
SB00023_MSB122102	SB00022_MSB122110	17934	0.159697	0.00039	0.301088
SB00022_MSB122110	SB00008_MVZ195115	17892	0.157501	0.000727	0.301227
SB00025_MSB127011	SB00023_MSB122102	18466	0.17405	0.006769	0.305086
SB00025_MSB127011	SB00015_MVZ195116	18930	0.164659	0.003909	0.306005
SB00018_MSB122109	SB00008_MVZ195115	18044	0.166482	0.002716	0.307564
SB00019_MSB122105	SB00017_MSB122108	17928	0.166053	0.000558	0.308357
SB00021_MSB122101	SB00020_MSB122104	18355	0.172596	0.000926	0.309948
SB00019_MSB122105	SB00018_MSB122109	18196	0.168334	0.000605	0.311704
SB00015_MVZ195116	SB00014_MSB122107	18311	0.175086	0.002184	0.31395
SB00025_MSB127011	SB00022_MSB122110	18524	0.164651	0.00054	0.313984
SB00020_MSB122104	SB00019_MSB122105	18351	0.181843	0.004032	0.317934
SB00020_MSB122104	SB00017_MSB122108	18183	0.173349	0.00066	0.318895
SB00020_MSB122104	SB00018_MSB122109	18451	0.180641	0.000325	0.33244